

CERES_EBAF_Ed4.2 and Ed4.2.1

Data Quality Summary

Version 5

Released 5/1/2025

Investigation: **CERES**

Data Product: **EBAF**

Data Set: **Terra (Instruments: CERES-FM1 or CERES-FM2)**
Aqua (Instruments: CERES-FM3 or CERES-FM4)
NOAA-20 (Instrument: CERES-FM6)

Data Set Version: **Edition4.2** **Release Date: January 2, 2024**
Edition4.2.1 TOA **Release Date: November 25, 2024**
Edition4.2.1 Surface **Release Date: March 14, 2025**

CERES Visualization, Ordering and Subsetting Tool: <https://ceres.larc.nasa.gov/data/>

This document provides a high-level quality assessment of the CERES Energy Balanced and Filled (EBAF) data product. As such, it represents the minimum information needed by scientists for appropriate and successful use of the data product. For a more thorough description of the methodology used to produce EBAF, please see Loeb et al. (2018, 2024) and Kato et al. (2018). It is strongly suggested that authors, researchers, and reviewers of research papers re-check this document for the latest status before publication of any scientific papers using this data product.

Notes to Users:

- To ensure you are using the latest version of EBAF, please check the version and release date in the netCDF file you have against the version and release date in this Data Quality Summary.

TABLE OF CONTENTS

<u>Section</u>	<u>Page</u>
1.0 Introduction.....	1
1.1 EBAF Product Description.....	1
2.0 Cautions and Helpful Hints.....	3
3.0 EBAF Edition4.2.....	7
3.1 Motivation for EBAF Ed4.2.....	7
3.2 Using regional climatology adjustments to transition between satellite records	7
3.3 The total solar irradiance dataset for the EBAF Ed4.2 product	9
3.4 EBAF Ed4.2 major algorithm improvements	10
3.5 EBAF Ed4.2 minor changes.....	11
3.6 Issues that affect surface fluxes.....	12
3.6.1 Surface albedo correction	12
3.6.2 MERRA-2 near air temperature and skin temperature trends	13
4.0 EBAF Edition4.2.1.....	16
4.1 Motivation for the EBAF Ed4.2.1 product.....	16
4.2 EBAF Ed4.2.1 changes	17
4.3 TOA flux differences between Ed4.2.1 and Ed4.2	18
4.3.1 Due to sampling inconsistencies.....	18
4.3.2 Due to bug fixes	21
4.3.3 Due to nighttime clear-sky footprint sampling differences	22
4.4 Cloud property differences between Ed4.2.1 and Ed4.2.....	23
4.4.1 Arctic polar night cloud property differences.....	23
4.4.2 Cloud property differences due to sampling inconsistencies.....	26
4.5 Surface flux improvements from Ed4.2 to Ed4.2.1.....	28

TABLE OF CONTENTS

<u>Section</u>	<u>Page</u>
4.5.1 Aerosol optical thickness correction for surface fluxes	28
5.0 Version History	30
6.0 References	31
7.0 Attribution.....	33
8.0 Feedback and Questions.....	34
9.0 Document Revision Record	35

1.0 Introduction

This document outlines the differences between EBAF Edition4.2 and Edition4.1 (Section 3.0) as well as EBAF Edition4.2.1 and EBAF Edition4.2 (Section 4.0). The Cautions and Helpful Hints (Section 2.0) apply to both editions. For reference, the EBAF Edition 4.1 Data Quality Summary is provided [here](#).

Edition 4.2:

Reason for edition change: To transition from Terra and Aqua to the NOAA20-only record due to the Terra and Aqua drifting orbits. Uses climatology adjustments to tie the Terra-only and NOAA-20-only periods to the Terra-Aqua record.

Period not affected: July 2002 to March 2022 same as Ed4.1.

Periods impacted: March 2000 to June 2002 and April 2022 to July 2024.

Edition4.2.1:

Reason for edition change: Input switch to MERRA-2 from GEOS5.4.1 atmosphere.

Period not affected: March 2000 to March 2022 same as Ed4.2.

Period impacted: April 2022 onward. Users can compare the Ed4.2.1 fluxes and clouds with Ed4.2 between April 2022 to July 2024.

1.1 EBAF Product Description

CERES Energy Budget and Filled (EBAF) dataset is produced using measurements from several instruments. It involves CERES and MODIS instruments flying on the Terra (descending sun-synchronous orbit with an equator crossing time of 10:30 A.M. local time) and Aqua (ascending sun-synchronous orbit with an equator crossing time of 1:30 P.M. local time) as well as geostationary imagers that provide hourly diurnal information between 60°S-60°N. Each CERES instrument measures filtered radiances in the shortwave (SW; wavelengths between 0.3 and 5 μm), total (TOT; wavelengths between 0.3 and 200 μm), and window (WN; wavelengths between 8 and 12 μm) regions. Unfiltered SW, longwave (LW) and WN radiances are determined following Loeb et al. (2001) and radiance-to-flux conversion uses empirical Angular Distribution Models from Su et al. (2015a). CERES instruments provide global coverage daily, and monthly mean regional fluxes are based upon complete daily samples over the entire globe. Cloud properties are determined from MODIS and geostationary imager measurements (Minnis et al. 2020). For detailed descriptions of how TOA and surface radiative fluxes in EBAF are generated, please see Loeb et al. (2018, 2024) and Kato et al. (2018, 2025).

Despite recent improvements in satellite instrument calibration and the algorithms used to determine SW and LW outgoing top-of-atmosphere (TOA) radiative fluxes, a sizeable imbalance persists in the average global net radiation at the TOA from CERES satellite observations. With the most recent CERES Instrument calibration improvements, the SYN1deg_Edition4 net imbalance is $\sim 4.3 \text{ W m}^{-2}$, much larger than the expected observed ocean heating rate $\sim 0.71 \text{ W m}^{-2}$ (Johnson et al. 2016). This imbalance is problematic in applications that use Earth Radiation Budget (ERB) data for climate model evaluation, estimations of the Earth's annual global mean energy budget, and studies that infer meridional heat transports. *The EBAF dataset uses an objective constraint algorithm to adjust SW and LW TOA fluxes within their ranges of uncertainty to remove the inconsistency between average global net TOA flux and heat storage*

in the Earth-atmosphere system.

A second problem users of standard CERES Level 3 data products have noted is the occurrence of gaps in monthly mean clear-sky TOA flux maps due to the absence in some $1^\circ \times 1^\circ$ regions of cloud-free areas occurring at the CERES footprint scale (~20-km at nadir). As a result, clear-sky maps from CERES SSF1deg contain many missing regions. In EBAF, the problem of gaps in clear-sky TOA flux maps is addressed by inferring clear-sky fluxes from both CERES and Moderate Resolution Imaging Spectrometer (MODIS) measurements to produce a clear-sky TOA flux in each $1^\circ \times 1^\circ$ region every month. In addition to the clear-sky flux determined only for the cloud-free portions of a region provided in Ed4.0, EBAF Ed4.1 and subsequent editions also include clear-sky flux estimates for the total region, which includes the cloudy portions. These clear-sky fluxes are defined in a manner that is more in line with how clear-sky fluxes are represented in climate models. These clear-sky fluxes are used to determine Cloud Radiative Effect (CRE). Loeb et al. (2020) describes the methodology used to determine the new clear-sky flux estimates for total regions.

The EBAF product provides seamless transitions from the Terra-only record (March 2000 to June 2002) to the Terra&Aqua record (July 2002 to March 2022) and then to the NOAA20-only record (April 2022 to present). To mitigate the flux and cloud discontinuities between records, the CERES EBAF Ed4.2 product applies regional climatology adjustments based on the 5-year overlap periods. The single satellite records are tied to the Terra&Aqua record. The TOA observed fluxes, imager cloud properties, and computed surface fluxes use climatology adjustments to facilitate trend analysis over the EBAF record. See Section 3.2 in this document, Loeb et al. (2024), and Kato et al. (2025) for more information on the climatology adjustment method.

2.0 Cautions and Helpful Hints

The CERES Science Team notes several CAUTIONS and HELPFUL HINTS regarding the use of CERES_EBAF_Ed4.2 (including EBAF_Ed4.2.1):

- TOA and surface Cloud Radiative Effects (CREs) in EBAF Ed4.2 are determined using the new clear-sky fluxes determined for the total region. This differs from EBAF Ed4.0, which determined CRE using clear-sky fluxes determined from cloud-free portions of a region only.
- The CERES_EBAF_Ed4.2 product can be visualized, subsetting, and ordered from: <https://ceres.larc.nasa.gov/data/>.
- The Aqua satellite experienced an anomaly preventing any data transmittal from August 16 to September 3, 2020. CERES processing for Edition4.2 and Ed4.2.1 used NOAA-20 only (climatologically adjusted) for the whole month of August. September 1-3 was not filled.
- Global means are determined using zonal geodetic weights. The zonal geodetic weights can be obtained from (<https://ceres.larc.nasa.gov/data/general-product-info/#geodetic-zone-weights-information>).
- Climatological mean values are determined for a base period of July 2005 – June 2015.

(a) **TOA Fluxes:**

- Users are cautioned that all-sky SW and LW TOA fluxes are determined from Terra only from March 2000-June 2002, combined Terra and Aqua for July 2002-March 2022, and NOAA-20 for April 2022 onwards. Clear-sky TOA fluxes are derived from Terra prior to July 2002, and Aqua thereafter until April 2022 onwards, which are based on NOAA-20.
- **This bullet pertains to Edition4.2 only; the issue has been corrected in Edition4.2.1.**
The monthly means of regional clear-sky LW are based on both daytime and nighttime observations. Regions with large diurnal clear-sky LW fluctuations, such as interior Australia, the Atacama Desert, Namibia, and the Sahel, were impacted by using incorrect clear-sky LW narrowband-to-broadband coefficients that severely limited the nighttime sampling of partial footprint clear-sky LW fluxes from the associated imager. These regions have anomalously larger clear-sky LW fluxes than the surrounding regions, since they were only based on daytime observations. This error only impacts the April 2022 to January 2024 data months. For December 2023 and January 2024, large outliers of clear-sky LW fluxes were identified and removed at the regional level. These regions were then spatially filled from surrounding regions. Beginning with the data month February 2024, the correct coefficients were used, and consequently the climatological adjustments were updated (Section 3.2). These corrections eliminated most of the anomalous regional clear-sky LW fluxes.
- In determining monthly mean cloud free area clear-sky SW TOA fluxes from daily mean values, the daily mean SW fluxes are weighted by the gridbox clear area fraction in order to minimize the influence of cloud contamination on the monthly mean clear-sky SW TOA flux. In contrast, daily mean clear-sky LW TOA fluxes are weighted equally when computing gridbox monthly mean values.
- Since TOA flux represents a flow of radiant energy per unit area and varies with distance from the earth according to the inverse-square law, a reference level is also needed to define satellite-based TOA fluxes. From theoretical radiative transfer calculations using a model that accounts for spherical geometry, the optimal reference level for defining TOA fluxes in radiation budget studies for the earth is estimated to be approximately 20 km. At this

reference level, there is no need to explicitly account for horizontal transmission of solar radiation through the atmosphere in the earth radiation budget calculation. In this context, therefore, the 20-km reference level corresponds to the effective radiative “top of atmosphere” for the planet. Since climate models generally use a plane-parallel model approximation to estimate TOA fluxes and the earth radiation budget, they implicitly assume zero horizontal transmission of solar radiation in the radiation budget equation and do not need to specify a flux reference level. By defining satellite-based TOA flux estimates at a 20-km flux reference level, comparisons with plane-parallel climate model calculations are simplified since there is no need to explicitly correct plane-parallel climate model fluxes for horizontal transmission of solar radiation through a finite atmosphere. For a more detailed discussion of reference level, please see Loeb et al. (2002).

- When the solar zenith angle is greater than 90° , twilight flux (Kato and Loeb 2003) is added to the outgoing SW flux to account for the atmospheric refraction of light. The magnitude of this correction varies with latitude and season and is determined independently for all-sky and clear-sky conditions. In general, the regional correction is less than 0.5 W m^{-2} , and the global mean correction is 0.2 W m^{-2} . Due to the contribution of twilight, there are regions near the terminator in which outgoing SW TOA flux can exceed the incoming solar radiation. Users should be aware that in these cases, albedos (derived from the ratio of outgoing SW to incoming solar radiation) exceed unity.
- EBAF uses geodetic weighting to compute global means. The spherical Earth assumption gives the well-known $S_0/4$ expression for mean solar irradiance, where S_0 is the instantaneous solar irradiance at the TOA. When a more careful calculation is made by assuming the Earth is an oblate spheroid instead of a sphere, and the annual cycle in the Earth's declination angle and the Earth-sun distance is taken into account, the division factor becomes 4.0034 instead of 4. The following file provides the zonal geodetic weights used to determine global mean quantities.
(<https://ceres.larc.nasa.gov/data/general-product-info/#geodetic-zone-weights-information>).
- Starting with the data date of August 2021, a supplemental dataset used to fill gaps in the microwave snow and ice data within 50 km of coasts (including large lakes and seas) changed to a higher resolution product, resulting in differences in those snow/ice maps. [Figure 2-1](#) shows differences due to this change in the all-sky and clear-sky TOA SW and LW fluxes from SSF1deg-Ed4A-Aqua run for January 2021. The differences are restricted to coastlines and are generally less than 5 W m^{-2} .

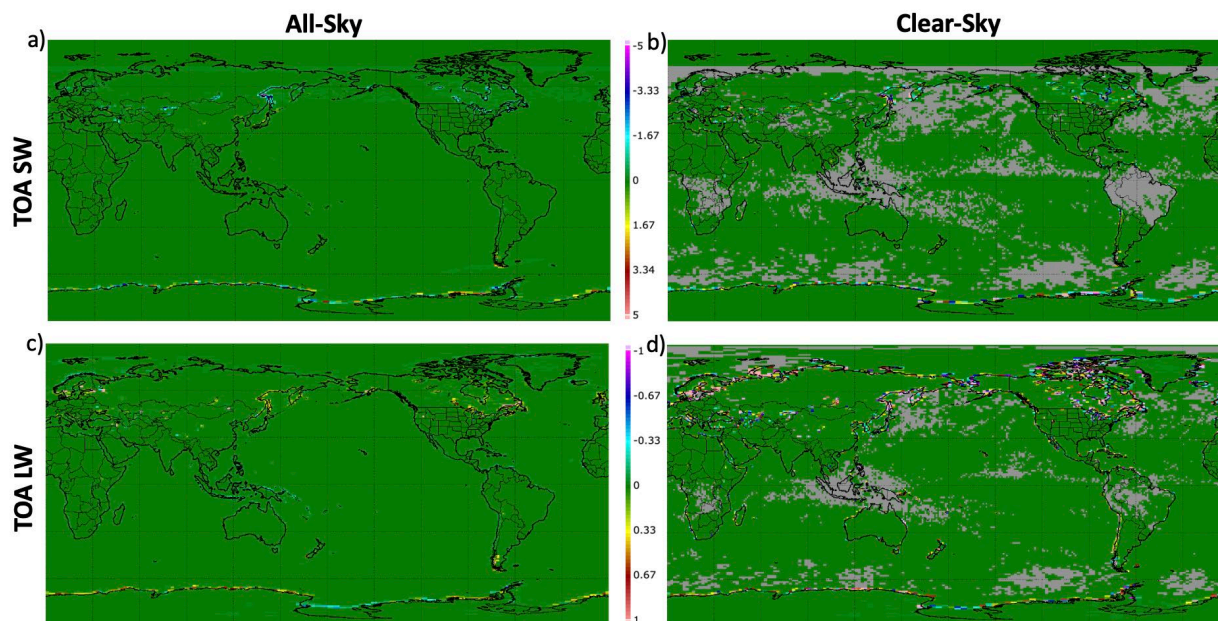


Figure 2-1. Differences in SSF1deg Ed4A monthly mean TOA fluxes (W m^{-2}) in January 2021 due to the change in the supplemental snow/ice dataset.

(b) Cloud Properties:

- Users are cautioned that imager-based cloud properties are determined from Terra only from March 2000-June 2002, combined Terra and Aqua for July 2002-March 2022, and NOAA-20 for April 2022 onwards. *Therefore, cloud properties may exhibit a discontinuity in July 2002 and in April 2022 owing to imager calibration differences and diurnal cloud property differences between the periods that may be unresolved with the cloud property climatological adjustment. See Section 3.2.*
- Because the Aqua MODIS 1.6 μm channel failed shortly after launch, the 1.24 μm channel is used as an alternative in both Aqua and Terra Ed4.2 daytime cloud optical depth retrievals over snow. However, the 1.24 μm channel is not optimal for cloud optical depth since surface reflectance can affect retrievals more than the 1.6 μm channel. Surface shortwave downward flux validation of radiative transfer results over Dome C using 1.6 μm and 1.24 μm cloud retrievals anecdotally suggest that the 1.24 μm cloud optical depths over snow are too large by several percent.
- The Terra-MODIS water vapor (6.76- μm) and the 8.55- μm channels have degraded since 2008, leading to some artificial trends in cloud properties that are most significant over polar regions (day and night) and non-polar oceans (nighttime). Corrections were made after the Terra spacecraft anomaly event (February 18-28, 2016) in an attempt to restore these channels to pre-degradation levels. As a result, some cloud properties also exhibit a sharp discontinuity and inconsistency before and after the Terra spacecraft anomaly over Antarctica and the Arctic Ocean during daytime and nighttime, and over the non-polar oceans during nighttime. The TOA SW and LW fluxes are not significantly affected.

(c) Surface Fluxes:

- Cloud radiative effects are computed as all-sky flux minus clear-sky flux.
- The net flux is positive when the energy is deposited to the surface, i.e. the net is defined as downward minus upward flux.
- There are regions where the surface flux adjustments are large, such as over the Andes, Tibet, and central eastern Africa. As a result, the deseasonalized anomalies over these regions can be noisy.
- Because the GEOS-5.4.1 skin temperatures were inadvertently used in Edition 4.2 instead of the MERRA-2 skin temperatures, when the regional trend of surface net longwave flux is computed over the Amazon, the magnitude of the trend is unphysically large.
- Because the degradation of Terra water vapor channels affected cloud retrievals starting around 2008, downward longwave flux anomalies over polar regions show a downward trend. Therefore, trend analyses with surface fluxes over polar regions using from Ed4.2 EBAF-Surface should be avoided. This problem was mitigated in Ed4.2.1.
- Although the frequency of occurrence of a positive net shortwave cloud effect or a negative net longwave cloud effect is rare, they are not entirely absent when cloud free area clear-sky fluxes are used for the cloud effect calculation. A possible reason that these apparently unphysical cloud radiative effects occur is because of a mismatch of sampling between all-sky and clear-sky. For example, if clear-sky is sampled during daytime more often than during nighttime, the net clear-sky longwave flux is less negative than the net clear-sky longwave flux with a uniform sample throughout a month. Therefore, when the less negative clear-sky net longwave flux is subtracted from all-sky net longwave flux, which is also generally negative, the resulting net longwave cloud effect can be negative. For shortwave over polar region where the solar zenith angle changes rapidly over the course of a month, if clear-sky samplings occur when solar zenith angle is large and a smaller net clear-sky shortwave flux is subtracted from all-sky net shortwave flux, the cloud effect can be positive.
- To ensure surface and TOA fluxes are consistent, Lagrange multiplier processes are used to adjust the MODIS or VIIRS cloud properties within uncertainty to ensure flux computations at TOA are consistent with those observed at TOA. The surface flux is then recomputed using the adjusted cloud properties (see Kato et al., 2018 for more details).
- MERRA-2 uses a coarse sea surface temperature and sea ice concentration data source through March 2006. Consequently, near surface and skin temperatures through March 2006 tend to be higher for some regions for both Ed4.2 and Ed4.2.1. Trends computed from April 2006 are not affected by these coarse resolution sources (See Section 3.6.2).
- The GEOS-5.4.1 sea surface temperature is used in Ed4.2 for the entire period. In Ed4.2.1, the GEOS-5.4.1 sea surface temperature is used from March 2000 through March 2022, and the MERRA-2 sea surface temperature is used from April 2022 onward.
- Under clear-sky conditions, the imager-derived skin temperature over land is used for surface flux computations. Temperature and humidity profiles used for the cloud algorithm to identify clear scenes are shown in Figure 4-1. Under cloudy conditions, skin temperature from the reanalysis used for the cloud algorithm is used for surface flux computations.

3.0 EBAF Edition4.2

3.1 Motivation for EBAF Ed4.2

The EBAF Ed4.2 product combines the a) Terra only record from March 2000 to June 2002, b) the Terra & Aqua record July 2002 to March 2022, and c) the NOAA-20-only record from April 2022 onward (Loeb et al. 2024). The transition from the Terra and Aqua record to a NOAA-20-only record was prompted by the Terra and Aqua orbits drifting outside of their maintained 15-minute local equator crossing time. The Terra and Aqua spacecraft have begun orbital maneuvers in 2021 to exit their respective orbits and are slowly drifting towards terminator orbits reaching 9AM and 3PM local equator crossing times in 2026. An Aqua spacecraft anomaly in early April 2022, which caused MODIS WV channel anomalies, accelerated the transition to a NOAA-20 record. The corrected WV calibration coefficients will be available in MODIS Collection 7.

The SSF1deg product monthly regional fluxes will be impacted by the changing Terra and Aqua orbital drifts. The SSF1deg product accounts for the diurnal variation by assuming constant meteorology to compute the 24-hour average fluxes. Many regions have systematic diurnal cycles, where the clouds decrease during the day (maritime stratus regions) or where the clouds increase during the afternoon (land afternoon convective regions). For these regions, changing the local crossing time would impact the monthly mean fluxes as the Terra and Aqua orbits start to drift and would therefore impact the long-term regional flux trends. Even a 15-minute drift can result in a SW monthly regional flux changes of 2 Wm^{-2} based on 15-minute Geostationary Earth Radiation Budget (GERB) studies ([see presentation here](#)). Since the EBAF product relies on the long-term flux regional flux stability of the SSF1deg product, the decision was made to transition to a NOAA-20-only EBAF record beginning in April 2022.

Beginning in April 2022, the Edition4A SYN1deg product will transition from a Terra, Aqua and hourly geostationary (GEO) dataset to a Terra, NOAA-20 and hourly GEO dataset. The SYN1deg dataset provides the diurnal asymmetry factors (DAR) needed to apply the diurnal SW models to the CERES SSF1deg SW all-sky observations. The SYN1deg all-sky LW fluxes are the basis for EBAF LW all-sky fluxes. The resulting SYN1deg product LW fluxes should not be impacted by the Terra drifting orbits, since the daily averaged fluxes are mostly based on the hourly GEO fluxes, which are carefully normalized regionally with the CERES fluxes. Once the Terra satellite is decommissioned, the SYN1deg product will transition to a NOAA-20 and hourly GEO dataset.

3.2 Using regional climatology adjustments to transition between satellite records

The Terra & Aqua period is considered the most diurnally accurate part of the EBAF record, since the Terra (10:30 MLT) and Aqua (1:30 MLT) observations provide most of the regional diurnal information supplemented by a small geostationary-derived flux contribution (Loeb et al 2018 and Loeb and Doelling 2020). The Terra-only and NOAA-20 (1:30MLT) records rely more on the geostationary-derived fluxes to estimate the daily flux means. To mitigate the flux discontinuity between Terra-only and Terra & Aqua records, the CERES EBAF Ed4.2 product applies regional climatology adjustments to the Terra-only record (March 2000 to June 2002) based on 5-years of overlap (July 2002 to June 2007). Calendar month dependent monthly mean flux climatology is computed over the overlap period. The adjustment applied to a calendar month for the Terra-only record is the mean difference of corresponding calendar months over the overlap period. The Terra-only EBAF dataset is processed during the overlap period to compute the

regional climatology adjustment,

$$\hat{F} = F(Terra) + [\bar{F}(Terra\&Aqua) - \bar{F}(Terra)] \quad (1)$$

where \hat{F} is the flux with the climatological adjustment, $F(Terra)$ and $F(Terra \& Aqua)$ are fluxes for, respectively, the Terra-only and Terra & Aqua periods, and the overbar indicates the climatological monthly mean fluxes computed for the 5-year overlap period. The bracketed term on the right side of Eq. (1) is the climatological adjustment. The regional climatology adjustment is used for both TOA and surface fluxes and is explained in Loeb et al. (2024). Similarly, for the NOAA-20-only record (beginning in April 2022) the climatology is based on the May 2018 to March 2022 overlap period. SW and LW flux regional climatology adjustments were computed for both all-sky and clear-sky conditions. For TOA fluxes, the regional flux climatology adjustments were not applied if the year-to-year monthly Terra & Aqua minus Terra-only flux standard deviation or dispersion was greater than 20%. The regional clear-sky flux climatology adjustments were only utilized if all years during the overlap period had valid clear-sky fluxes (from either observed CERES footprints or MODIS narrowband to broadband fluxes) before spatial filling. The SW climatology adjustment was not applied if the resulting SW flux was less than 0.0 Wm^{-2} . To ensure that the climatology adjustments did not impact the regional and global trends, the trend of the climatologically adjusted NOAA-20-only minus the Terra & Aqua fluxes during the overlap period was found to be much smaller than the overall Terra & Aqua trend (Loeb et al. 2024). Similarly, the climatologically adjusted NOAA-20-only minus the Terra & Aqua fluxes during the overlap period monthly regional or global anomalies were also found to be smaller than the overall Terra & Aqua anomalies. This validates that the flux regional climatology adjustments are not introducing any artificial trends or anomalies in the EBAF Ed4.2 record; the analysis can be found in Loeb et al. (2024) for TOA fluxes and in Kato et al. (2025) for surface fluxes. The EBAF Ed4.1 dataset did incorporate clear-sky flux climatology adjustments during the Terra-only record but did not incorporate all-sky flux or cloud climatology adjustments. [Table 3-1](#) describes the climatology adjustment strategy as a function of satellite record. The timeline is also shown in [Figure 3-1](#).

The cloud properties given to the user in the EBAF product were also climatologically adjusted. The cloud properties were cloud-fraction weighted to obtain the cloud climatology adjustments. No regional cloud property climatology adjustments were made over regions that did not have valid cloud property observations for each year during the overlap period. The cloud climatology adjustments were not applied if the resulting cloud fraction, cloud effective temperature, cloud effective pressure, and cloud optical depth was less than 0%, 200K, 200hPa, 0.05 or greater than 100%, 310K, 980hPa, 40, respectively.

Table 3-1. Satellite data record range and associated climatology adjustment strategy.

Data Range	TOA Clear-sky fluxes	TOA All-sky fluxes	Cloud properties
03/2000 – 06/2002	Terra ^a	Terra ^c	Terra ^c
07/2002 – 03/2022	Aqua	Terra+Aqua	Terra+Aqua
04/2022 – onwards	NOAA-20 ^b	NOAA-20 ^d	NOAA-20 ^d

^a Adjusted so that 07/2002-06/2007 climatology matches Aqua's

^b Adjusted so that 05/2018-03/2022 climatology matches Aqua's

^c Adjusted so that 07/2002-06/2007 climatology matches Terra+Aqua's

^d Adjusted so that 05/2018-03/2022 climatology matches Terra+Aqua's

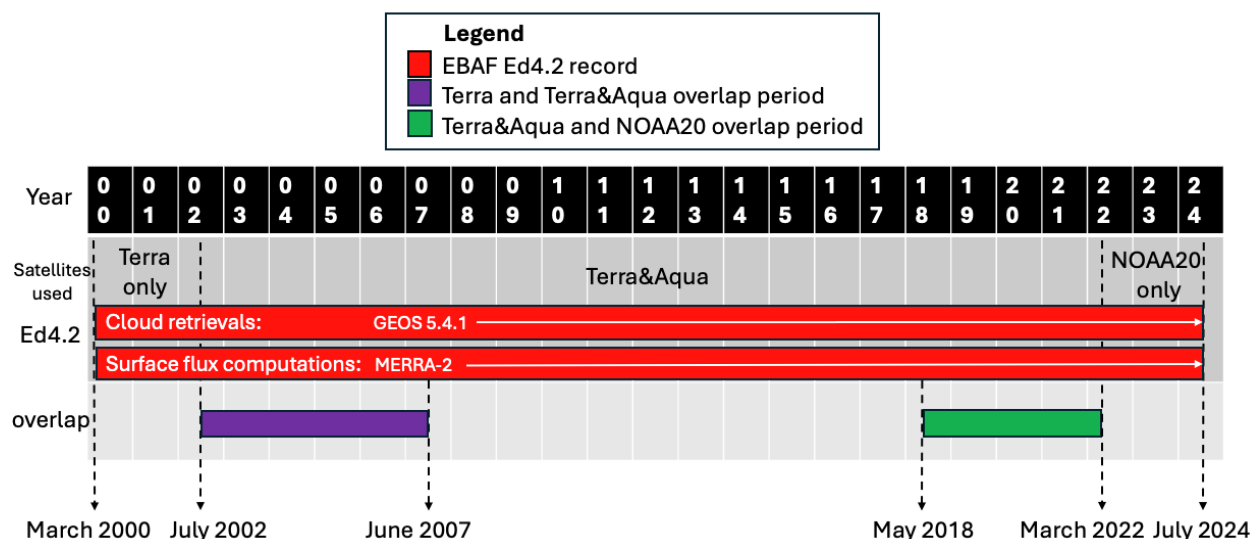


Figure 3-1. A schematic of the EBAF Ed4.2 CERES instrument satellite platforms and the GEOS 5.4.1/MERRA-2 reanalysis input timelines along with the overlap periods used to compute the Terra-only and NOAA-20-only climatology adjustments.

3.3 The total solar irradiance dataset for the EBAF Ed4.2 product

The EBAF Edition 4.1 total solar irradiance (TSI) reference was based on Solar Radiation and Climate Experiment (SORCE) version 15, which was used between 25Feb2003 to 30Jun2013. The WRC composite (Mar2000 to 24Feb2003), RMIB composite (01Jul2013 to 31Oct2014), SORCE/TSIS-1 composite (01Jan2018 to 25Feb2020) and [TSIS-1/TIM V3](#) beginning in 25Feb 2020 TSI datasets were radiometrically scaled to the SORCE V15 calibration. More information regarding the EBAF Ed4.1 TSI is found [here](#). The solar community has a new TSI composite that combines TSI sensor records and is known as the community consensus TSI dataset; it was created by G. Kopp using the methodology of Dudok de Wit et al. (2017). The daily community consensus TSI composite can be accessed [here](#). Since the community consensus TSI dataset has a longer lag time than the near-real time EBAF product, the TSIS-1/TIM V3 is appended to the community consensus TSI data beginning with May 7, 2022. The TSIS-1/TIM V3 is first radiometrically scaled to the community consensus record, utilizing the previous 100 days of overlap to determine the scaling factor. The EBAF Ed4.2 global TSI record mean is $\sim 0.16 \text{ Wm}^{-2}$ greater than the corresponding Ed4.1 value (see [Figure 3-2](#)). The EBAF product was energy balanced using the same Ed4.1 ocean heat storage value and based on the same 10-year period between July 2005 and June 2015, avoiding the single satellite periods. The resulting EBAF Ed4.2 minus Ed4.1 global net flux record mean difference (March 2000 to March 2022) is less than 0.02 Wm^{-2} .

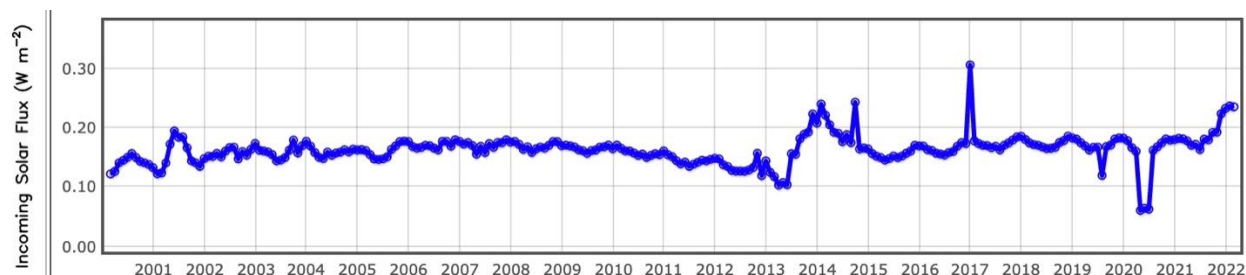


Figure 3-2. The EBAF Ed4.2 minus Ed4.1 total solar incoming difference.

3.4 EBAF Ed4.2 major algorithm improvements

- Fixed the diurnal asymmetry ratio (DAR) coding bug. DAR is computed by taking the morning minus afternoon SW flux ratio from the SYN1deg product. DAR should be computed in local time but was mistakenly computed in GMT, which resulted in pairing the afternoon flux and the morning flux of the following local day. This caused large spurious values of DAR near the dateline (Loeb and Doelling 2020 and [here](#)). DAR is used to compute the SW diurnal corrections applied to the SSF1deg product to compute the EBAF SW monthly mean regional fluxes.
- The EBAF product estimates clear-sky SW and LW fluxes in mostly overcast regions, which contain no clear-sky CERES observed footprints, by applying narrowband to broadband coefficients to the MODIS channel radiances within the clear portion of CERES partly cloudy footprints (Loeb et al. 2018). The MODIS narrowband to broadband coefficients are based on regressions of matched clear-sky footprint MODIS channel and CERES radiances. The MODIS-derived broadband radiances are then converted to fluxes using the CERES angular directional models (ADMs) and corrected to match the observed footprint clear-sky fluxes. The EBAF Ed4.1 narrowband to broadband coefficients were based on MODIS collection 5 across the entire record regardless of the MODIS collection used. For EBAF Ed4.2, the MODIS or VIIRS narrowband to broadband coefficients are based on the collection (C) number that is consistent with imager version used in the CERES record. MODIS C5 coefficients were applied between 2000 and February 2016, MODIS C6.1 coefficients were applied between March 2016 and March 2022, and NOAA-20 VIIRS C2.1 coefficients are applied beginning in April 2022. See [Table 3-2](#) to note the MODIS and VIIRS collection timelines used in the CERES record.

Table 3-2. The imager and collection used to compute the imager-derived clear-sky fluxes.

Data range	03/2000- 06/2000	07/2002-02/2016	03/2016-03/2022	04/2022-onwards
Imager & collection	Terra-MODIS C5	Aqua-MODIS C5	Aqua-MODIS C6.1	NOAA-20-VIIRS C2.1

- Edition 4.2 EBAF is processed based on Edition 4 SYN1degree. Edition 4 SYN1degree uses multiple sources of surface albedo. The surface albedo history map approach is used when cloud amount is less than a threshold value. For cloudy scenes, other approaches are used.

Because surface albedos derived from other approaches are less accurate than surface albedo derived by the surface albedo history map approach, we decided to apply a correction to albedos derived by other approaches. See Section 3.6.1 for a discussion of the correction method.

3.5 EBAF Ed4.2 minor changes

- For October 2004, the EBAF Ed4.2 monthly mean fluxes are based on October 13 to 31 observations, whereas the EBAF Ed4.1 incorrectly based the monthly mean fluxes on all days in October. The Aqua-CERES instrument radiance observations saturated over bright Earth targets resulting in spurious fluxes over the first 12 days of the month. The instrument issue was resolved on October 13, 2004.
- From August 16 to September 3, 2020, the Aqua spacecraft experienced an anomaly. For EBAF Ed4.1, NOAA-20 observations were simply substituted for the missing days during the anomaly. For EBAF Ed4.2, the August 2020 monthly mean fluxes and clouds are based entirely on the NOAA-20-only climatology adjusted fluxes and clouds (like the NOAA-20-only record beginning in April 2022).
- The EBAF Ed4.1 product did not properly apply the SW flux twilight correction (Kato and Loeb 2003) to all December months. This correction accounts for the refracted SW flux over regions with solar zenith angles greater than 90°. EBAF Ed4.2 applied the SW flux twilight correction for all months.
- The EBAF Ed4.1 product incorporated spurious MODIS granules during August 18, 2000 (Terra-MODIS) and August 6, 2002 (Aqua-MODIS), resulting in noisy cloud property retrievals that impacted the ADM scene selection used to convert the CERES radiance to fluxes. EBAF Ed4.2 product did not utilize those days in its processing.
- During the early Terra-CERES record, data gaps greater than one week occurred during August 6-18, 2000, June 15-July 2, 2001, and March 20-28, 2002. The EBAF Ed4.2 utilized the SW and LW fluxes from the SYN1deg product for the days with no CERES observations over non-polar regions. The SYN1deg GEO-derived fluxes were carefully normalized with CERES observations that were available during other days of the month. Over polar regions (>60° in latitude), the monthly mean fluxes are based on days with data only. This enables a more accurate observed monthly mean flux to facilitate comparisons with climate models.
- The EBAF Ed4.1 product utilized MODIS C5 until March 2018 and transitioned to MODIS C6.1 beginning in April 2018 when MODIS C6.1 became available. MODIS C6.1 mainly addressed spurious WV channel issues that occurred after the Terra spacecraft anomaly (February 18-29, 2016) (Wilson et al. 2017). The entire MODIS C6.1 L1B record was reprocessed; however, the CERES project only reprocessed the SSF1deg and SYN1deg records using MODIS C6.1 between February 2016 and March 2018). EBAF Ed4.2 incorporated the updated February 2016 through March 2018 SSF1deg and SYN1deg records.
- A SYN1deg SW temporal interpolation error was fixed in EBAF Ed4.2 when GEO regions experience glint conditions that occur over tropical oceans. During glint conditions, no GEO SW fluxes are derived but are temporally interpolated between neighboring non-glint hourly GEO fluxes. A more accurate DAR is obtained by this proper SW interpolation.

- Both Edition 4.1 and Edition 4.2 surface fluxes are based on the SYN1deg-Month product, which contains hourly surface fluxes. In the Edition 4.1 product, all MODIS-, VIIRS-, and geostationary satellite-derived cloud properties are used for surface flux computations. Geostationary satellites provide hourly cloud properties outside the MODIS and VIIRS overpass times. In Edition 4.2, only MODIS- and VIIRS-derived cloud properties are used; no geostationary satellite-derived cloud properties are used. Cloud properties derived from MODIS and VIIRS are temporally interpolated in computing hourly fluxes. For the interpolation, clouds are separated into four types depending on cloud top pressure (Kato et al. 2018). Cloud properties that are interpolated include fraction, cloud top and base pressures, optical depth, particle (ice and liquid) size, and water phase (1 for liquid and 2 for ice).
- In the Edition 4.1 product, GEOS-5.4.1 provides temperature and humidity profiles for the surface flux computations. In Edition 4.2, MERRA-2 temperature and humidity profiles are used for surface flux computations (Figure 3-1). Edition 4.2 surface fluxes use clouds retrieved with the GEOS-5.4.1 temperature and humidity profiles.

3.6 Issues that affect surface fluxes

Surface albedos are derived from multiple algorithms depending on sky conditions. Accuracy of surface albedo depends on the algorithm used. To improve surface albedo accuracy and maintain consistency of albedo, we apply minor corrections to surface albedo in producing both Ed4.2 and Ed4.2.1 surface fluxes. These are discussed in Section 3.6.1.

Near surface air temperature affects downward longwave fluxes. Surface skin temperature affects upward longwave fluxes. Changes on the MERRA-2 data sources affect near surface air temperature and skin temperature through March 2006. Analysis of MERRA-2 near surface air temperature and skin temperature is presented in Section 3.6.2.

3.6.1 Surface albedo correction

Edition 4.2 EBAF is processed based on Edition 4 SYN1degree. Edition 4 SYN1degree uses multiple sources of surface albedo. The surface albedo history map approach is used when cloud amount is less than a threshold value. For cloudy scenes, other approaches are used. Because surface albedos derived from other approaches are less accurate than surface albedo derived by the surface albedo history map approach, we decided to apply a correction to albedos derived by other approaches. In this section we discuss the correction method.

The correction begins with estimating albedo contributions to surface downward and upward irradiances. To isolate surface albedo contributions to surface downward and upward shortwave irradiances, we use the method given by Stephens et al. (2015). The top-of-atmosphere reflected irradiance F_{TOA}^{\uparrow} is the sum of reflected shortwave by the atmosphere and transmitted irradiance from the surface,

$$F_{TOA}^{\uparrow} = rS + tF_{sfc}^{\uparrow}$$

where r and t are intrinsic reflectance and transmittance of the atmosphere. Similarly, the downward shortwave irradiance at the surface is the sum of the transmitted irradiance by the atmosphere and the reflected irradiance by the atmosphere,

$$F_{sfc}^{\downarrow} = tS + rF_{sfc}^{\uparrow}$$

When the system reflectance and transmittance are defined as $R = F_{TOA}^{\uparrow}/S$ and $T = F_{sfc}^{\downarrow}/S$, then

$$T = \frac{t}{1 - ra}$$

and

$$R = r + \frac{tat}{1 - ra}$$

where the surface albedo $a = F_{sfc}^{\downarrow}/F_{sfc}^{\uparrow}$. The intrinsic reflectance and transmittance of the atmosphere are, respectively,

$$t = T \frac{1 - aR}{1 - a^2T^2}$$

and

$$r = R - taT$$

We use intrinsic reflectance and transmittance from SYN1deg and use the surface albedo from surface albedo history map, a' , to compute the revised system transmittance

$$T' = \frac{t}{1 - ra'}$$

revised downward shortwave surface irradiance by

$$F_{sfc}^{\downarrow'} = ST'$$

revised upward shortwave surface irradiance by

$$F_{sfc}^{\uparrow'} = a'F_{sfc}^{\downarrow'}$$

and revised upward shortwave irradiance at TOA by

$$F_T^{\uparrow'} = rS + tF_{sfc}^{\uparrow'}$$

We apply this method to equal area grid daily using daily mean surface albedo.

3.6.2 MERRA-2 near air temperature and skin temperature trends

MERRA-2 temperature and humidity profiles are used to compute surface fluxes throughout the time series. Because EBAF Ed4.2 also used MERRA-2 temperature and humidity profiles for flux computations, air temperature and humidity trends in EBAF Ed4.2.1 are the same as those in EBAF Ed4.2.

Cloud retrievals for EBAF Ed4.2.1 use GEOS-5.4.1 from March 2000 through March 2022 and use MERRA-2 from April 2022 onward, while cloud retrievals for EBAF Ed4.2 use GEOS-5.4.1 throughout the time series (Figure 4-1). Surface albedos and surface skin temperatures under clear conditions are retrieved from clear-sky scenes. The retrieved surface albedos are used in surface flux computations by the method explained in Rutan et al. (2009). The retrieved surface skin temperatures replace reanalysis skin temperatures. Because clear scenes are identified by the cloud algorithm and the cloud mask depends on temperature and humidity profiles used in the retrieval, the EBAF Ed4.2.1 skin temperatures from April 2022 onward are different from the EBAF Ed4.2 skin temperatures for the same period.

The MERRA-2 skin temperatures have a known issue. Sea surface temperature (SST) and sea ice concentration (SIC) in MERRA-2 after year 2000 are derived from two sources: daily 1/4° data as in Reynolds et al. (2007) are used through March 2006, and daily 1/20° data from the Operational Sea Surface Temperature and Sea Ice Analysis (OSTIA) as in Donlon et al. (2012) are used from April 2006 onwards (Bosilovich et al. 2015). Because of the coarse resolution sources used through March 2006, the land skin temperatures and near surface air temperatures over land are slightly positively biased. As a consequence, trends of regional skin temperature and near surface temperatures over land are smaller or negative. When the trend is computed from April

2006, the bias in trends is mitigated. [Figure 3-3](#) and [Figure 3-4](#) show, respectively, regional 2m air temperature and skin temperature trends. For comparison, trends derived from ERA5 are also shown. Differences of the MERRA-2 air temperature trend over central Africa and Antarctic from ERA5 2m air temperature are apparent (top row, [Figure 3-3](#)). When trends are computed from April 2006, the differences are smaller (bottom row, [Figure 3-3](#)). Improvements in the skin temperature are less pronounced, but better agreements of skin temperature trends with ERA5 are seen over the Southern Ocean south of New Zealand ([Figure 3-4](#)) when trends are computed from April 2006.

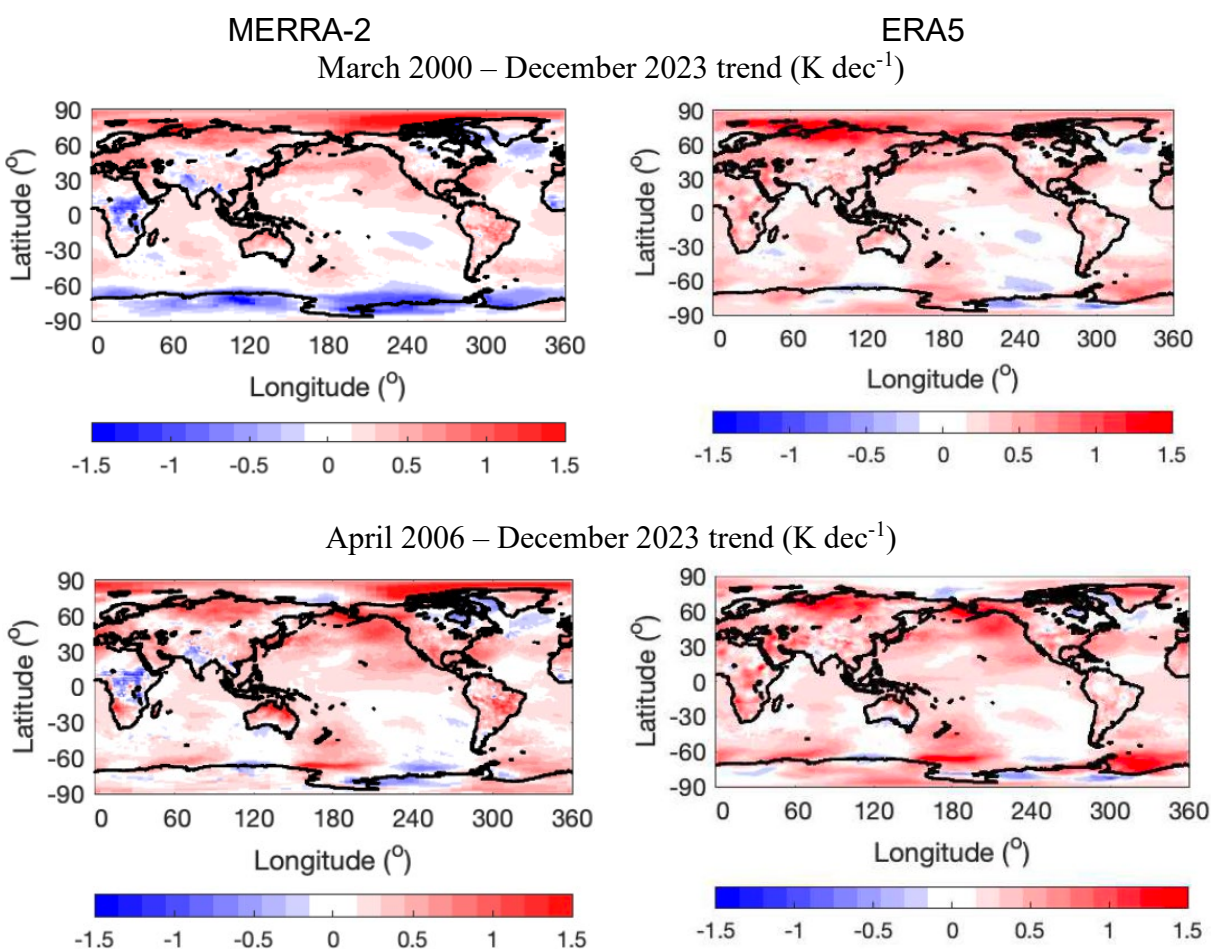


Figure 3-3. Regional 2m surface air temperature trend in K dec⁻¹ derived from left) MERRA-2 and right) ERA5 for the period from March 2000 through December 2023 (top row). Bottom row is the same as top except the period is from April 2006 through December 2023. Anomalies are computed from the July 2005 through June 2015 climatology.

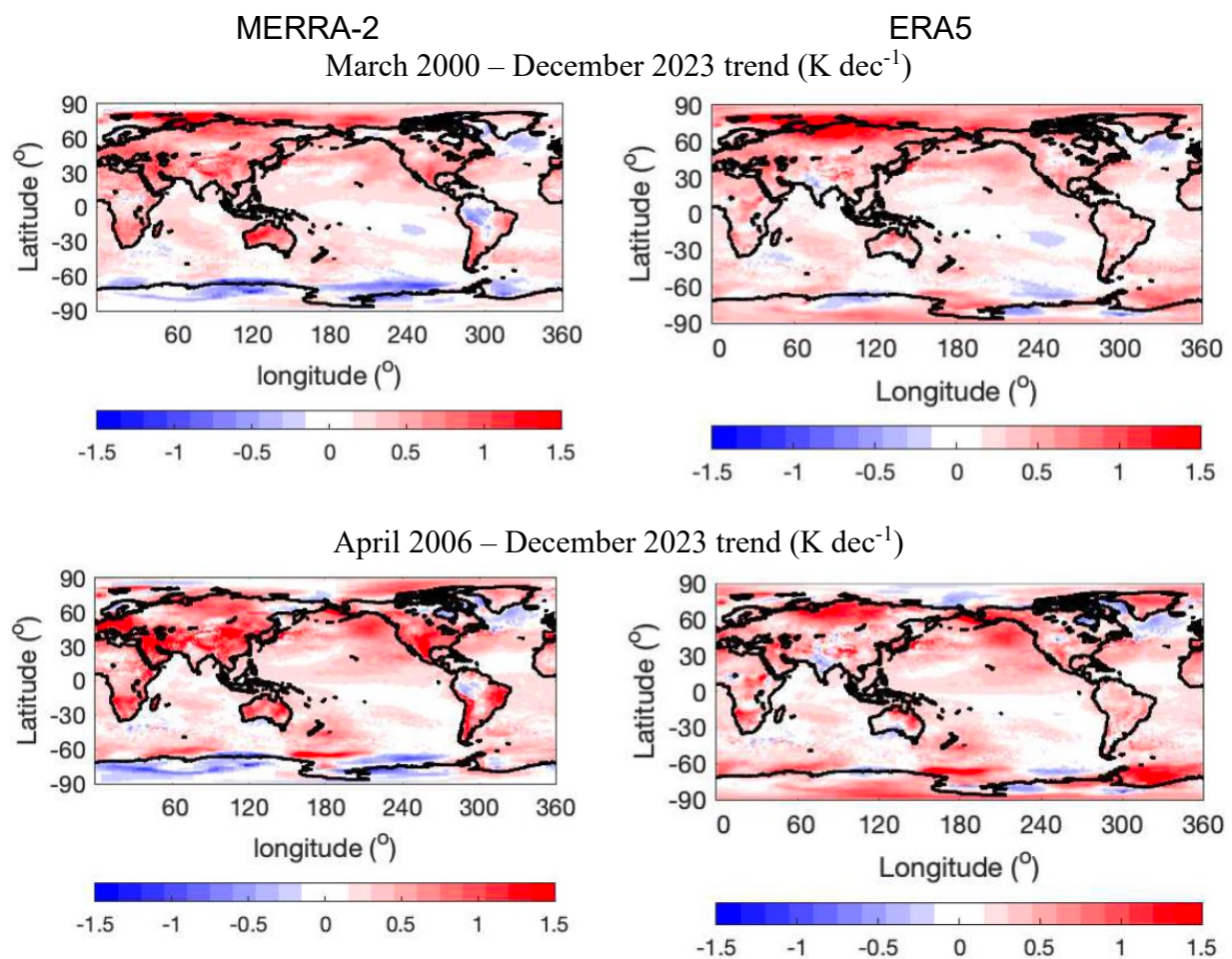


Figure 3-4. Same as [Figure 3-3](#) except for surface skin temperature.

4.0 EBAF Edition4.2.1

4.1 Motivation for the EBAF Ed4.2.1 product

The release of the EBAF Ed4.2.1 product was prompted by the discontinuation of the Goddard Space Flight Center (GSFC) Global Modeling and Assimilation Office (GMAO) Goddard Earth Observing System (GEOS5.4.1) (Reinicker et al. 2008) reanalysis dataset in July 2024, which had been used to provide the regional atmospheric profile data for the MODIS and VIIRS imager cloud mask and cloud retrievals. EBAF Ed4.2.1 utilizes the GMAO MERRA-2 reanalysis atmosphere (Gelaro et al. 2017, <https://gmao.gsfc.nasa.gov/reanalysis/MERRA-2/>) to retrieve the imager cloud properties beginning in April 2022 that are provided in the EBAF product. The cloud properties are also used to provide the scene type information for the CERES angular directional models (ADMs) (Su et al. 2015a, 2015b) utilized to convert the observed CERES instrument radiances into fluxes. The cloud properties are also utilized to select the regional SW diurnal models (Loeb et al. 2018) used to compute the regional 24-hour averaged daily SW fluxes from the instantaneous flux observations. Cloud properties are also used to compute the EBAF surface fluxes. In order to limit the number of times new inputs are introduced in the EBAF record, and rather than transitioning in August 2024, the MERRA-2 reanalysis is incorporated in the EBAF processing stream when the EBAF record transitioned from the Terra & Aqua record to the NOAA-20-only record in April 2022. The EBAF NOAA-20-only flux and cloud record (April 2022 to the present) is tied to the Terra & Aqua record (July 2002 to March 2022) utilizing regional climatology adjustments obtained during the Terra & Aqua and NOAA-20 4-year overlap period (May 2018 to March 2022) (see Section 3.2). Similar to the EBAF TOA observed fluxes, the EBAF Ed4.2.1 surface fluxes utilized climatology adjustments to transition between the Terra and Aqua GEOS5.4.1 imager cloud and the NOAA-20 VIIRS MERRA-2 cloud based records using the same overlap period.

Figure 4-1 illustrates the timeline for the Ed4.2.1 CERES instrument satellite platforms and reanalysis inputs. The EBAF Ed4.2.1 MERRA-2 reprocessing effort provided an opportunity to fix several coding bugs and to address sampling issues in Ed4.2 as well as to incorporate the MERRA-2 atmosphere used to derive cloud properties. Users can compare the EBAF Ed4.2 and Ed4.2.1 TOA fluxes and clouds between April 2022 and July 2024 to determine the impact of the atmospheric datasets. The CERES project has provided a [document](#) that quantifies the mostly insignificant impact of the Ed4.2.1 minus Ed4.2 regional TOA flux and cloud anomalies for January and July 2023 and associated global trends.

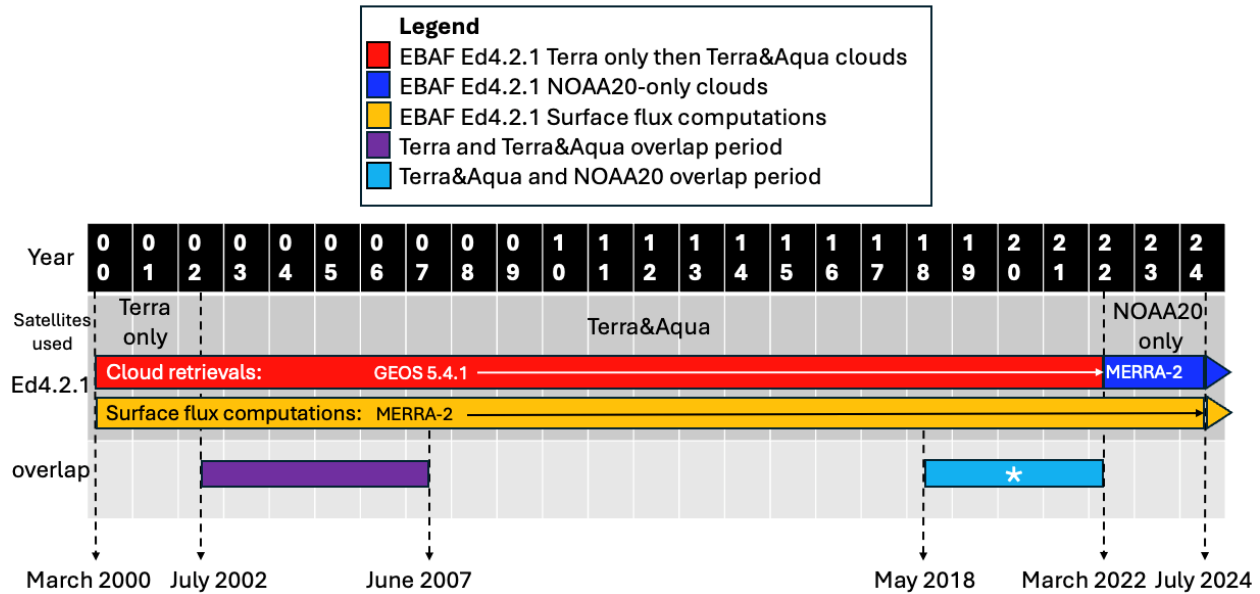


Figure 4-1. A schematic of the EBAF Ed4.2.1 CERES instrument satellite platforms and the GEOS 5.4.1/MERRA-2 reanalysis input timelines along with the overlap periods used to compute the Terra-only and NOAA-20-only climatology adjustments.

* The NOAA-20 in the blue overlap period uses MERRA-2 for both the cloud retrievals and surface flux computations, where the Terra&Aqua uses GEOS-5.4.1 for cloud retrievals and MERRA-2 for surface flux computations.

4.2 EBAF Ed4.2.1 changes

- We changed the atmospheric input to GMAO MERRA-2 from GEOS5.4.1 during the NOAA-20 only period beginning with April 2022 used to retrieve the imager cloud properties (Section 4.1). The resulting TOA flux differences are discussed in Section 4.3; the cloud property differences are discussed in Section 4.4.
- Ed4.2.1 processing has recovered some periods of missing data from Ed4.2 (Section 4.3.1).
- Ed4.2.1 used the correct narrowband to broadband coefficients to compute the clear-sky fluxes from partially clear footprints (Section 4.3.2).
- Discontinuities in imager-derived aerosol optical thicknesses caused by switching from MODIS to VIIRS are mitigated in producing Ed4.2.1 surface fluxes (Section 4.5.1).
- Edition4.2.1 surface fluxes use clouds retrieved with MERRA-2 for the NOAA-20-only period (Figure 4-1).

4.3 TOA flux differences between Ed4.2.1 and Ed4.2

4.3.1 Due to sampling inconsistencies

For EBAF, the 1:30 PM local time NOAA-20 CERES instantaneous SW flux observations are utilized to estimate the 24-hour mean SW flux using diurnal albedo models based on the associated imager cloud retrievals. The regional daily 24-hour mean fluxes are computed in local time and then parsed into a GMT-based month. The last day of the previous calendar month and the first day of the following calendar month are required to fully sample a GMT-based month. To facilitate a 2-month latency within real-time, the EBAF monthly forward processing does not include the first day of the following calendar month. However, when the record is reprocessed the first day of the following calendar month is included because it is now available. This mainly impacts the SW all-sky flux as shown in Figure 4-2. During April 2022, June 2022, September 2023, and July 2024, Ed4.2 also sampled the first day of the following calendar month similar to the EBAF Ed4.2.1 flux. The EBAF regional monthly all-sky LW flux does not require the first day of the following month since it incorporates the hourly GEO-derived broadband fluxes between $\pm 60^\circ$ in latitude.

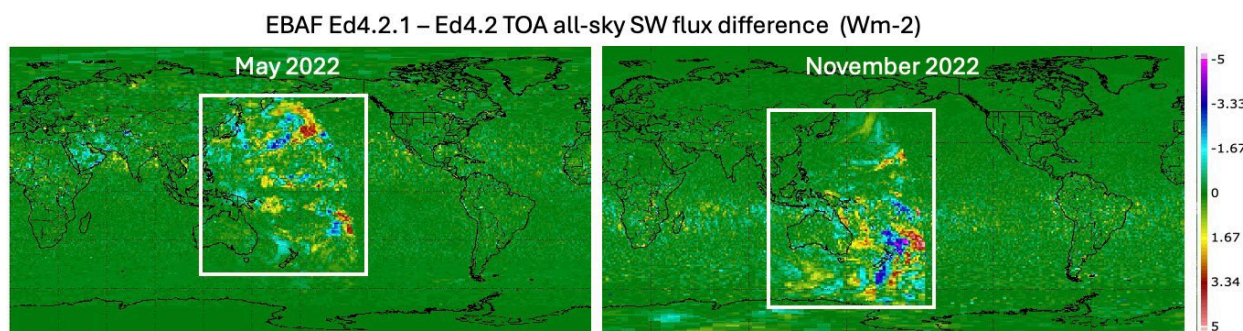


Figure 4-2. The EBAF Ed4.2.1 minus Ed4.2 TOA all-sky SW flux difference in Wm^{-2} shows the impact (denoted by the white box near the dateline) of not using the first day of the following calendar month in the EBAF Ed4.2 product. The EBAF Ed4.2.1 utilized the first day of the following month to compute the regional monthly all-sky SW flux.

Occasionally, some additional NOAA-20 CERES instrument or VIIRS imager data is recovered after the near real-time monthly releases of the EBAF Ed4.2 TOA product. Also, some flagged NOAA-20 CERES or VIIRS imager data was inadvertently processed and later deleted from the CERES archive. The EBAF Ed4.2.1 properly processed the NOAA-20 CERES instrument and VIIRS imager data. The periods with NOAA-20 Ed4.2.1 and Ed4.2 sampling differences are highlighted in Table 4-1. There are NOAA-20 data gaps common to both Ed4.2.1 and Ed4.2 (last column) that will not be reflected in the Ed4.2.1 and Ed4.2 flux and cloud differences; however, they may impact the EBAF record during these months.

Table 4-1. Dates and GMT ranges of the sampling inconsistencies in the NOAA-20 CERES record. *Partial* denotes a small fractional hour difference within the GMT hour indicated. *All GMT 0-24* denotes a major sampling difference encompassing the entire day, where the date is shown in bold. The EBAF NOAA-20-only record begins in April 2022 and is denoted by the double line. Sampling differences prior to April 2022 may have impacted the climatology adjustments computed from the overlap period.

Date	EBAF Ed4.2 missing data filled in Ed4.2.1	EBAF Ed4.2 data not in Ed4.2.1	Data gaps in both Ed4.2 and Ed4.2.1
July 19, 2018			All GMT 5-15
August 17, 2018	Partial GMT 3, 15		
January 1, 2019	Partial GMT 6		
July 3, 2021		Partial GMT 14	
February 10, 2022		Partial GMT 6	
February 16, 2022		Partial GMT 11	
December 9, 2022		Partial GMT 10	
December 13, 2022		Partial GMT 2	
March 1, 2023		Partial GMT 11	
March 29, 2023	All GMT 0-24		
September 29 to October 1, 2023			September 29 GMT 19 to October 1 GMT 13
January 18-19, 2024			January 18 GMT 18 to January 19 GMT 24
February 1, 2024	All GMT 0-24		
February 3-5, 2024			February 3 GMT 18 to February 5 GMT 17
February 20, 2024	GMT 16-20		
February 25, 2024		Partial GMT 5	
May 2, 2024	All GMT 0-24		
July 17, 2024		Partial GMT 13	

The largest sampling difference between Ed4.2 and Ed4.2.1 occurs in February 2024. [Table 4-1](#) shows that the entire day of February 1 was missing from the EBAF Ed4.2 record as well as 5 hours during February 20. For February 2024 both Ed4.2.1 and Ed4.1 had an additional 48-hour period missing between February 3 to 5. Essentially 1.2 out of 27 days missing in EBAF Ed4.2 are available in Ed4.2.1. Both March 2023 and May 2024 had 1 missing day out of 31 days.

[Figure 4-3](#) illustrates the flux impact of the Ed4.2 missing day in February 2024 when compared with the neighboring month of January 2024, which only shows the impact of the GEOS5.4.1 and MERRA-2 atmosphere datasets. The regional monthly all-sky flux averages are computed from days that contain a CERES observation. The all-sky SW flux dateline feature is due to not incorporating the first day of the following month into the monthly mean (see [Figure 4-2](#)). The all-sky LW flux is a combination of NOAA-20 LW fluxes and hourly GEO-derived broadband fluxes between $\pm 60^\circ$ latitude that have been regionally normalized to the NOAA-20 LW fluxes. The GEO-derived broadband LW fluxes do not utilize any cloud property scene type information and strictly use only the GEO water vapor and window channel radiances, which have been radiometrically scaled to the imager channel radiances, to derive the broadband LW flux. Therefore, the all-sky LW fluxes are not impacted by sampling or atmosphere dataset differences. However, over the poles, the LW flux is based on NOAA-20 CERES LW flux measurements that

are linearly interpolated in time and may be impacted by sampling differences. The clear-sky monthly SW and LW fluxes are not based on the daily means, but are determined on a monthly basis. The clear-sky SW flux difference over the Antarctic is more than likely due to clear-sky Ed4.2.1 and Ed4.2 coverage differences. The clear-sky LW flux is minimally impacted by the change in atmospheric dataset, except for a slightly larger impact for winter months over the Amazon basin. See Section 4.3.3 for further explanation.

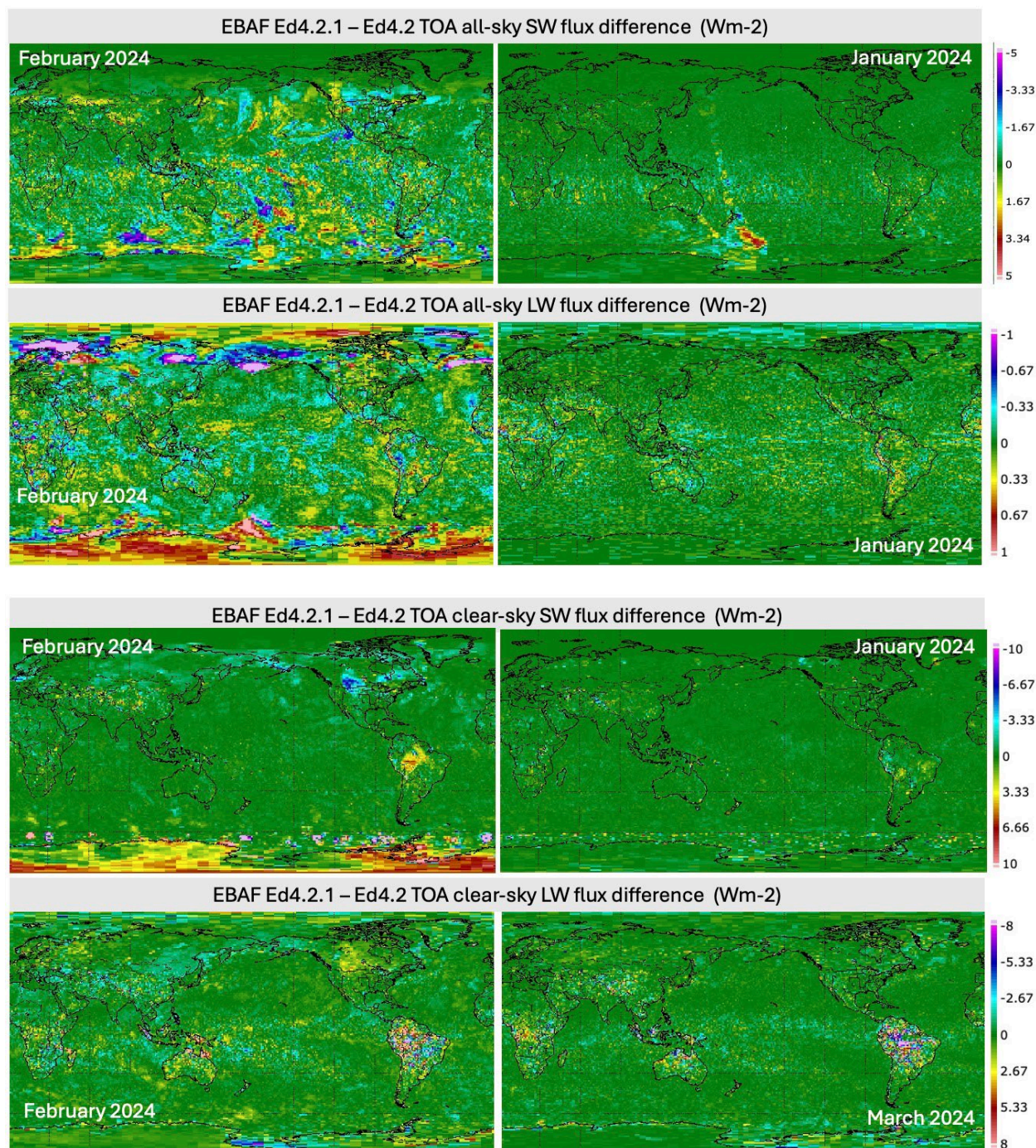


Figure 4-3. (left panels) The Ed4.2.1 minus Ed4.2 all-sky SW flux (top panel), all-sky LW flux (2nd row panel), clear-sky SW flux (3rd row panel), clear-sky LW flux (bottom panel) differences due to missing Ed4.2 data in 2024 February 1 (24 hours) and 20 (5 hours) that was filled in Ed4.2.1 (see Table 4-1). The February 3-5 data gap affected both Editions. The right panels display the impact of the MERRA-2 and GEOS5.4.1 atmosphere datasets. The February 2024 all-sky SW flux difference is due to the forward processing sampling difference between Ed4.2 and Ed4.2.1 (see Section 4.3.1).

4.3.2 Due to bug fixes

The EBAF TOA clear-sky SW and LW fluxes incorporate both clear-sky and partly cloudy CERES instrument footprints, where the partly cloudy footprint clear-sky flux contribution is based on imager narrowband to broadband relationships. The imager narrowband to broadband look up table (LUT) coefficients are derived from the clear-sky footprint dataset and applied to the clear-sky portion of the partly cloudy footprints. For EBAF Ed4.2 between April 2022 and February 2024, an incorrect NOAA-20 LUT was implemented. The EBAF Ed4.2.1 product used the correct NOAA-20 LUT. This mainly impacted the clear-sky LW coefficients, whereas the clear-sky SW LUT coefficients were nearly identical. The clear-sky LW flux impact is dependent on month. Figure 4-4 (left panel) shows the EBAF Ed4.2.1 (with the correct LUT) minus the Ed4.2 (with incorrect LUT) clear-sky LW flux difference. Figure 4-4 (right panel) shows the EBAF Ed4.2.1 minus the Ed4.2 clear-sky LW flux difference where both EBAF editions used the same LUT, thus highlighting only the impact of the GEOS and MERRA-2 atmosphere differences on the clear-sky LW flux. The larger clear-sky LW flux differences over tropical land afternoon convective regions are explained in Section 4.3.3.

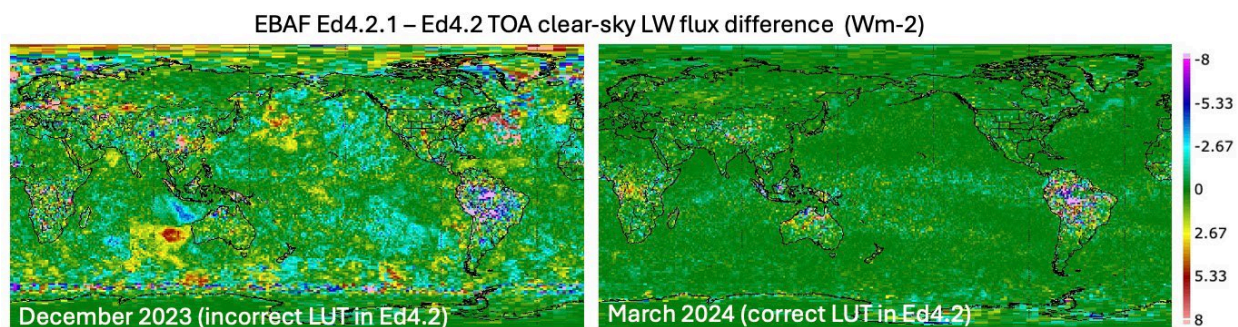


Figure 4-4. (left panel). The December 2023 EBAF Ed4.2.1 (with correct LUT) minus Ed4.2 (with incorrect LUT) TOA all-sky SW flux difference in Wm^{-2} . (right panel). The EBAF Ed4.2.1 minus March 2024 Ed4.2 TOA all-sky SW flux difference in Wm^{-2} where both editions are using the correct LUT.

An EBAF NOAA-20 coding bug did not set the clear-sky fraction to zero over glint regions when applying the CERES shortwave ADM. Both the EBAF Ed4.2.1 and Ed4.2 were processed with this coding bug until February 2024. The coding bug was fixed for Ed4.2.1 beginning with March 2024; however, the older Ed4.2 version was processed with the coding bug. The Figure 4-5 (left panel) shows the impact of the GEOS and MERRA-2 atmosphere difference on the all-sky SW fluxes, which are minimal, where both the EBAF Ed4.2 and Ed4.2.1 product were processed

with the same coding bug. Figure 4-5 (right panel) shows the impact of the coding bug, which impacted the all-sky SW flux difference within the white rectangle, where Ed4.2.1 was processed correctly and Ed4.2 had the bug. Unfortunately, the coding bug was present during the Terra & Aqua and NOAA-20 overlap period which was used to compute the climatology adjustments. However, the impact to the climatology adjustments should be insignificant.

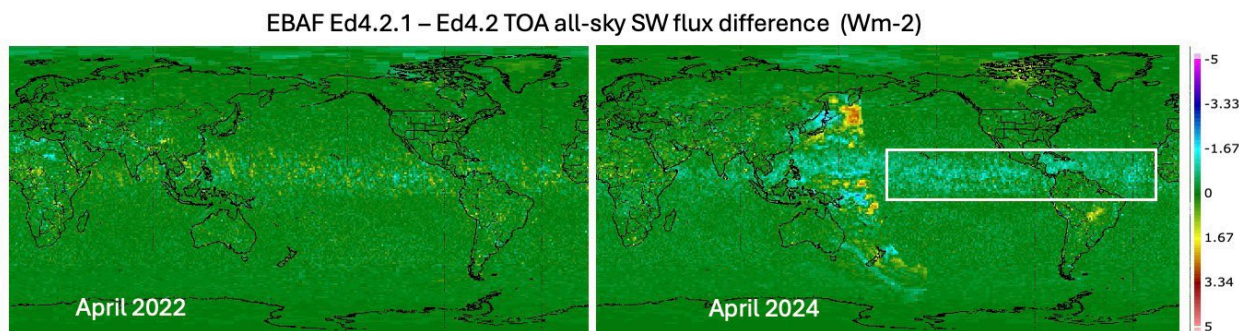


Figure 4-5. (left panel) The EBAF Ed4.2.1 (with coding bug) minus Ed4.2 (with coding bug) TOA all-sky SW flux difference in Wm^{-2} , highlighting the MERRA-2 and GEOS5.4.1 atmosphere difference on the all-sky SW flux. (right panel) The EBAF Ed4.2.1 (coding bug fixed) minus Ed4.2 (with coding bug) TOA all-sky SW flux difference in Wm^{-2} . The coding bug differences are illustrated within the white box; the dateline difference is due to not processing the first day of the following month (see Section 4.3.1).

4.3.3 Due to nighttime clear-sky footprint sampling differences

The EBAF clear-sky LW and SW fluxes are a combination of clear-sky identified footprints and the clear portion of the partly cloudy footprint fluxes. Imager narrowband to broadband coefficients based on the clear-sky identified footprints are used to estimate the clear-sky flux from the partly cloudy footprints. The daytime cloud mask is based on both visible and IR imager channels; however, for nighttime, only the IR imager channels are utilized. Thus the nighttime cloud mask relies more on the atmospheric profile and surface skin temperature. The Ed4.2 NOAA-20 VIIRS imager cloud mask utilized the GEOS5.4.1 atmosphere and skin temperatures, whereas the Ed4.2.1 used the MERRA-2 atmosphere and skin temperatures between April 2022 and July 2024. Over land, both daytime and nighttime clear-sky LW fluxes are required to estimate the regional monthly clear-sky LW flux, since the EBAF algorithm employs a half-sine shape, which peaks at local noon and is constrained by the night observations, to estimate the diurnal land heating. If there are no nighttime clear-sky LW observations, then the half-sine algorithm cannot be implemented, and that region is assigned a default clear-sky LW flux. The default regions are then filled spatially from neighboring regions to provide the EBAF product's spatially complete regional clear-sky fluxes.

To compute regional clear-sky LW climatology adjustments for a given month, every year during the overlap period (May 2018 to March 2022) must have a valid clear-sky LW flux. Very cloudy tropical land regions may not have a valid monthly clear-sky LW flux. During the NOAA-20 record beginning in April 2022, these non-adjusted regions revealed greater Ed4.2.1 and Ed4.2

clear-sky LW differences as seen over the Amazon basin in November 2023 and February 2024 in Figure 4-6. This mainly impacts the Amazon basin during the winter months.

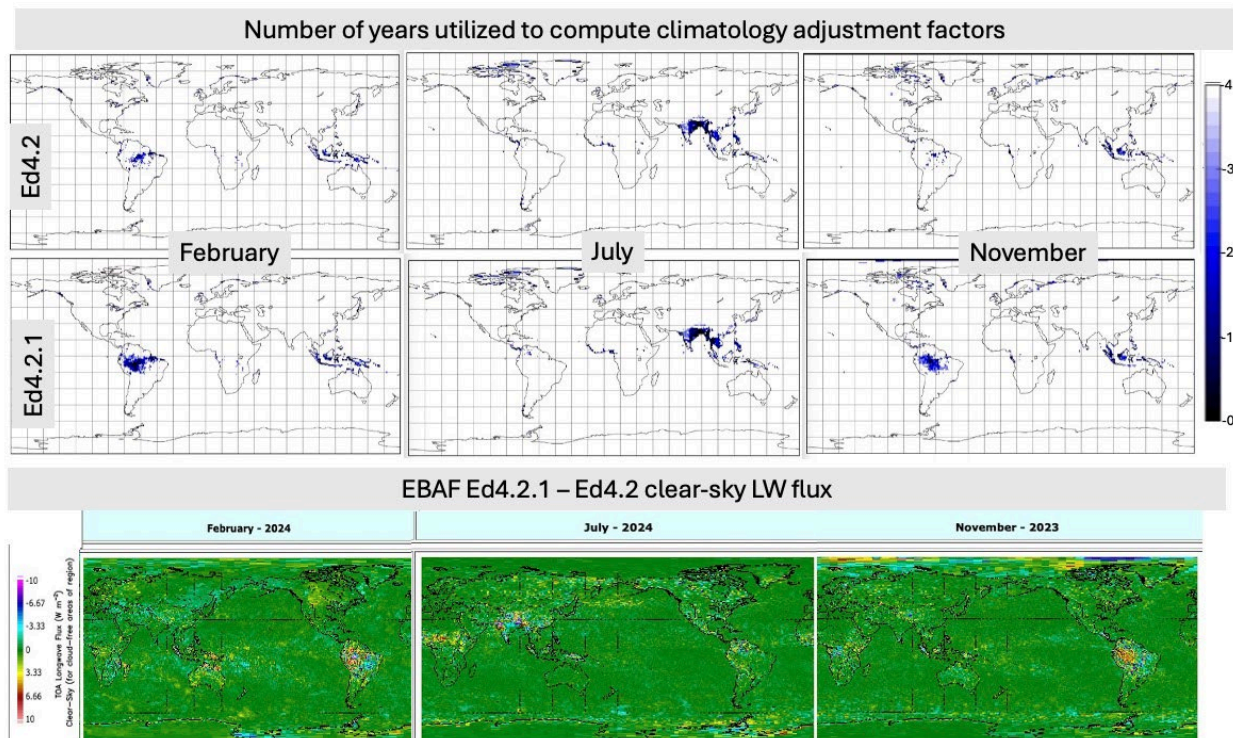


Figure 4-6. (top panel). The EBAF Ed4.2 number of years with valid clear-sky LW fluxes for the months of February, July, and November month during the overlap period (May 2018 to March 2022). Climatology adjustments are only computed if all 4 years are available during the overlap period. (middle panel) The EBAF Ed4.2.1 number of years with valid clear-sky LW fluxes. (bottom panel) The EBAF Ed4.2.1 minus Ed4.2. clear-sky LW flux difference for February 2024, July 2024, and November 2023, where the greatest difference is associated with the difference in Ed4.2.1 and Ed4.2 number of available years.

4.4 Cloud property differences between Ed4.2.1 and Ed4.2

This section discusses differences in the climatologically adjusted cloud properties between Ed4.2.1 and Ed4.2. The EBAF product cloud properties are climatologically adjusted to allow the users to monitor the “true” long-term cloud trends in the CERES records without being encumbered by input or retrieval algorithm variations. These climatologically adjusted cloud properties are given in the EBAF product for the convenience of the user. These are NOT the cloud properties used to derive the TOA fluxes, total clear-sky TOA fluxes, or computed surface fluxes.

4.4.1 Arctic polar night cloud property differences

Regional climatology adjustments were designed to combine consistently retrieved cloud satellite imager records. However, any spurious cloud retrievals during the imager overlap period may be propagated by the climatology adjustments and would impact the EBAF product clouds in the NOAA20 only record. The GEOS5.4.1 Arctic polar night skin temperature during the overlap

(May 2018 to March 2022) differed from the NOAA20 period (April 2022 to present). The difference in Arctic polar night skin temperature impacted the cloud retrievals. The MERRA-2 regional skin temperature over Arctic polar night is up to 8K warmer than the corresponding GEOS5.4.1 skin temperature (see [Figure 4-7](#)) between 2019 and 2022. The MERRA-2 minus GEOS5.4.1 skin temperature is much smaller during 2022 and 2023 because the GEOS5.4.1 had a skin temperature input dataset change on November 7th, 2022. The GEOS5.4.1 skin temperatures were based on the weekly Reynolds sea surface temperature and sea ice product that was discontinued in November 2022, after which the GEOS5.4.1 utilized the daily NOAA Optimum Interpolation Sea Surface Temperature (OISST) product for skin temperature. The MERRA-2 uses the daily Operational Sea Surface Temperature and Sea Ice Analysis (OSTIA) system provided by the Met Office. The OISST and OSTIA have more similar skin temperatures over the Arctic polar night.

Since the Arctic polar night atmosphere is very dry, the imager cloud mask is mostly dependent on skin temperature to identify the cloudy imager pixels. The warmer predicted TOA radiances based on the skin temperatures increased the NOAA-20 VIIRS MERRA-2 (Ed4.2.1) retrieved cloud fraction by up to 30% (see [Figure 4-8](#)). The cloud climatology adjustments were computed during the Terra & Aqua and NOAA-20 overlap period, which encompassed May 2018 through March 2022. The cloud climatology adjustments were then applied to the EBAF NOAA-20-only period beginning in April 2022. However, the MERRA-2 and GEOS5.4.1 skin temperature was more consistent after November 2022 than before November 2022. Skin temperature shift in GEOS-5.4.1 affect cloud properties used for Ed4.2. However, cloud properties used for Ed4.2.1 are not affected by the skin temperature shift. The cloud fraction adjustment derived from the overlap period was much larger than what was required for the NOAA-20-only period, causing a smaller Ed4.2.1 cloud fraction than for the Ed4.2 (see [Figure 4-9](#)). The Ed4.2.1 cloud effective pressure is greater than for Ed4.2; however, the cloud effective temperature was minimally impacted. The EBAF cloud optical depth is a daytime retrieval and therefore not impacted. Any effort to remove the overadjustment of cloud fraction in the polar nighttime regions from the EBAF record would probably adversely impact the EBAF cloud properties. The same is true for the Antarctic polar night; however, the MERRA-2-GEOS5.4.1 skin temperature difference is much smaller. The Ed4.2.1 minus Ed4.2 cloud fraction is negligible, and the cloud effective temperature and pressure differences are mostly within 5 K and 500 hPa (not shown) over both the continent and sea ice extent. The user should be aware of this artifact and not correlate the EBAF Arctic or Antarctic polar night cloud properties.

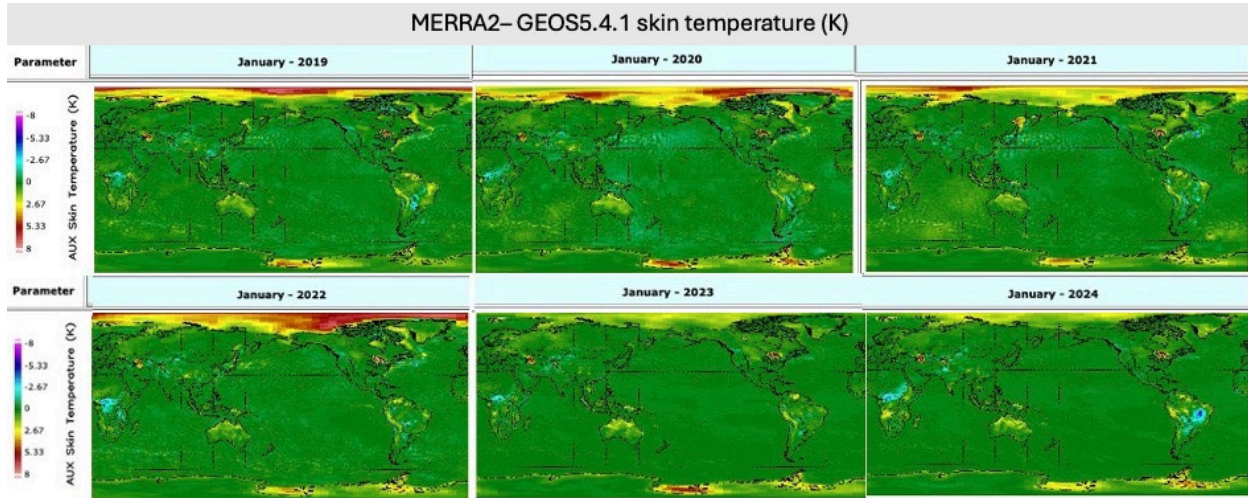


Figure 4-7. The January MERRA-2 minus GEOS5.4.1 skin temperature difference between 2019 and 2024. Note the larger Arctic skin temperature differences between 2019 and 2022 and smaller differences for 2023 and 2024. The difference is due to changes in GEOS5.4.1 during November 2022.

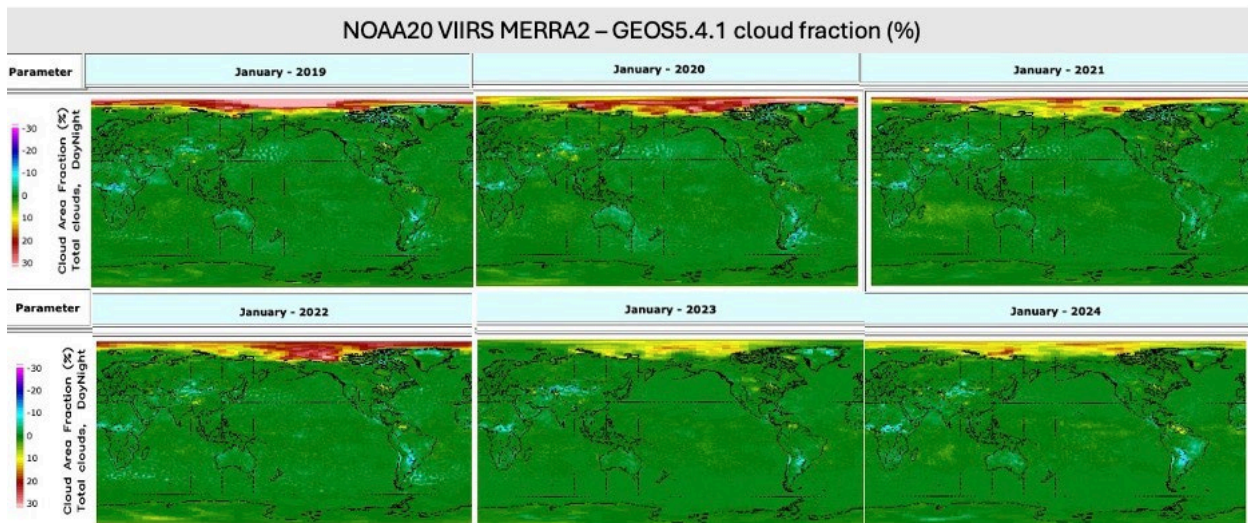


Figure 4-8. The January NOAA-20-VIIRS MERRA-2 minus GOES5.4.1 retrieved cloud fraction between 2019 and 2024. Note the larger Arctic cloud fraction differences between 2019 and 2022 and smaller differences for 2023 and 2024 due to the skin temperature difference shown in [Figure 4-7](#). The difference is due to changes in GEOS5.4.1 during November 2022.

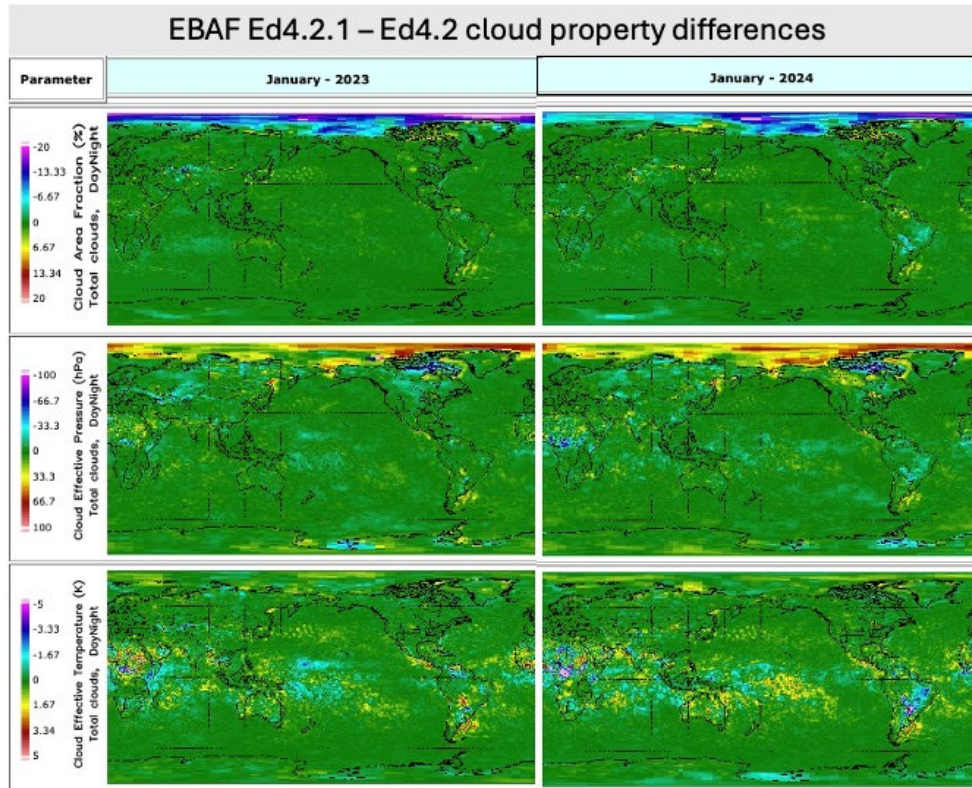


Figure 4-9. (top panel) The January 2023 and January 2024 EBAF Ed4.2.1 minus Ed4.2 cloud fraction difference in %, (middle panel) the cloud effective pressure difference in hPa, and (bottom panel) the cloud effective temperature difference in K. The Arctic cloud fraction can differ by up to 20% and the cloud effective pressure by 100hPa; however, the Arctic cloud effective temperature is not impacted.

4.4.2 Cloud property differences due to sampling inconsistencies

The cloud properties given in the EBAF product were also impacted by Ed4.2.1 and Ed4.2 sampling differences shown in [Table 4-1](#). The EBAF cloud fraction, effective temperature, and effective height are linearly interpolated in time between day and nighttime imager retrievals, whereas the logarithm of the cloud optical depth is linearly interpolated in time during the daytime only. If no observations are available for the day, then that day is not used to compute the monthly average from the daily means. During February 2024, 1.2 out of 27 days are missing in EBAF Ed4.2 that are available in Ed4.2.1 (see [Section 4.3.1](#)). [Figure 4-10](#) shows February Ed4.2.1 and Ed4.2 cloud property differences due to sampling inconsistencies compared to a neighboring month with consistent sampling. The Ed4.2.1 and Ed4.2 cloud property differences are due to the NOAA-20 imager cloud retrievals based on MERRA-2 or GEOS5.4.1 atmospheres and skin temperatures. For all cloud properties, sampling inconsistencies had a greater impact on the Ed4.2.1 and Ed4.2 cloud property differences than the atmosphere input (see [Figure 4-10](#)). The Arctic polar night differences are explained in [Section 4.4.1](#).

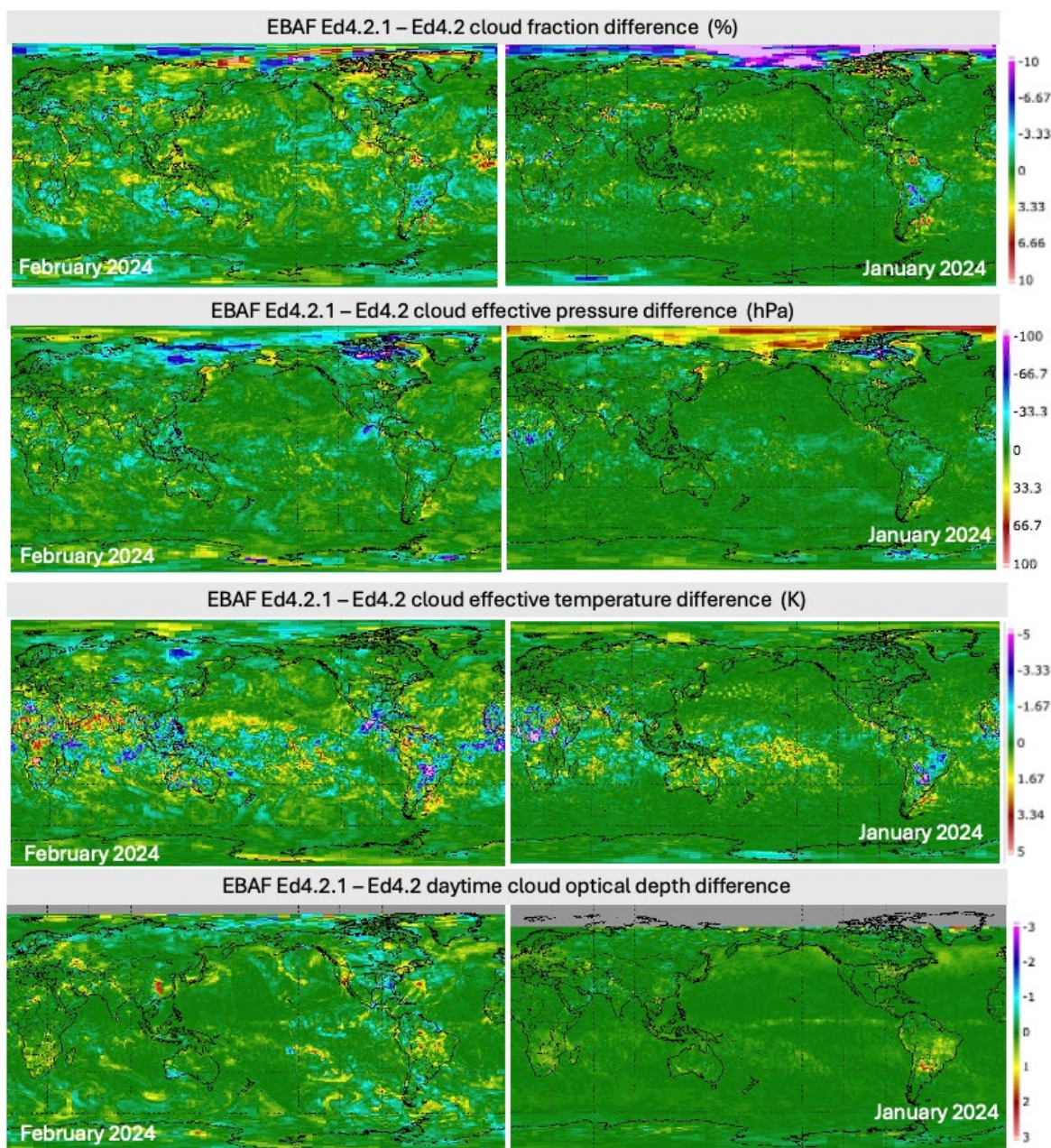


Figure 4-10. (left panels) The Ed4.2.1 minus Ed4.2 cloud fraction (%) (top panel), cloud effective pressure (hPa) (2nd row panel), cloud effective temperature (K) (3rd row panel), and cloud optical depth (bottom panel) difference due to sampling inconsistencies between Ed4.2 and Ed4.2.1 (see [Table 4-1](#)). The February 3-5 data gap affected both Editions. (right panels) Cloud differences that are not associated with sampling inconsistencies. The Arctic polar night cloud fraction and cloud effective pressure differences are explained in [Section 4.4.1](#).

4.5 Surface flux improvements from Ed4.2 to Ed4.2.1

Edition 4.2 and Ed421 surface fluxes from March 2000 through March 2022 are the same. Differences occur after April 2022. In Ed4.2.1, temperature and humidity profiles used for cloud retrieval and flux computations are consistent in the NOAA-20 only period (i.e. April 2022 onward, [Figure 4-1](#)). In addition, aerosol optical thickness discontinuities caused by transition from MODIS to VIIRS are mitigated by the method discussed in Section [4.5.1](#).

4.5.1 Aerosol optical thickness correction for surface fluxes

Aerosol optical thicknesses are corrected before used for Edition 4.2.1 EBAF surface product for the time period from April 2022 onward (NOAA-20 only period).

The source of aerosol optical thicknesses is Terra and Aqua MODIS from March 2000 through March 2022 and NOAA-20 VIIRS from April 2022 onward. For the MODIS period, aerosol optical thicknesses over ocean are derived by the Dark Target algorithm (Levy et al. 2013) and aerosol optical thicknesses over land are derived by the Dark Target and Deep Blue (Hsu et al. 2006) algorithms. For the VIIRS period, both Dark Target and Deep Blue algorithms are used for ocean and land.

Because of a revision of Deep Blue algorithm, aerosol optical thicknesses derived from VIIRS are significantly different from those derived from Terra and Aqua MODIS. To mitigate the discontinuity in aerosol optical thickness derived by the Deep Blue algorithm in the transmission from MODIS to VIIRS, we correct VIIRS derived aerosol optical thicknesses using coefficients provided by the Deep Blue team (Jaehwa Lee of University of Maryland). The coefficients depend on month, i.e. 12 sets of coefficients. In addition, we derived correction coefficients to aerosol optical thicknesses derived by the Dark Target algorithm overland. The coefficients over land were derived regressing Dark Target aerosol optical thicknesses derived from VIIRS with those derived from Aqua MODIS. The coefficients do not depend on time but depend on aerosol optical thickness. The optical thicknesses from 0 to 3.0 were divided into bins with 0.01 width and coefficients were derived for each bin separately. [Table 4-2](#) summarizes the use and corrections used for the Ed4.2.1 process.

Table 4-2. Algorithm and corrections to aerosol optical thickness used in the Edition 4.2.1 process.

	Dark Target	Correction	Deep Blue	Correction
Ocean				
Terra+Aqua	used	no	not used	no
NOAA20	used	no	used	yes
Land				
Terra+Aqua	used	no	used	no
NOAA20	used	yes	used	yes

The correction largely mitigates the difference of optical thicknesses derived from MODIS and VIIRS. However smaller differences exist ([Figure 4-11](#) and [Table 4-3](#)).

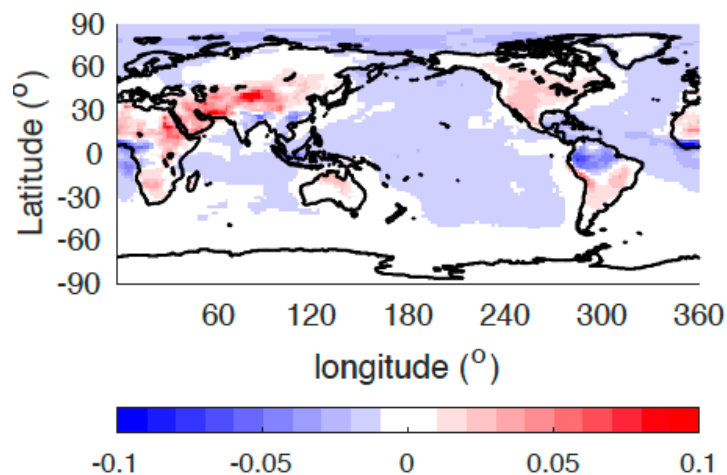


Figure 4-11. Difference of monthly mean aerosol optical thickness (VIIRS NOAA20 – MODIS Terra+Aqua) averaged from May 2018 to April. Both dark target and deep blue aerosols are used with corrections applied to VIIRS aerosol optical thicknesses.

Table 4-3. Global monthly mean aerosol optical thicknesses derived from Terra+Aqua MODIS and NOAA20 VIIRS observations.

	MODIS monthly mean optical thickness	VIIRS monthly mean optical thickness	VIIRS – MODIS optical thickness difference	Standard deviation of regional optical thickness differences
April 2022	0.1779	0.1753	-0.0026	0.0188
July 2022	0.1790	0.1780	-0.0010	0.0265
October 2022	0.1513	0.1480	-0.0033	0.0154
January 2023	0.1450	0.1407	-0.0043	0.0162

5.0 Version History

December 2022: Released Edition 4.2 EBAF TOA fluxes.

February 2023: Released Edition 4.2 EBAF Surface fluxes.

January 2024: Revised surface fluxes and TOA total area clear-sky fluxes from March 2000 through June 2023.

November 2024: Released Edition 4.2.1 EBAF TOA fluxes.

March 2025: Released Edition 4.2.1 EBAF computed surface and CRE fluxes.

6.0 References

- Bosilovich, M. G., S. Akella, L. Coy, R. Cullather, C. Draper, R. Gelaro, R. Kovach, Q. Liu, A. Molod, P. Norris, K. Wargan, W. Chao, R. Reichle, L. Takacs, Y. Vikhliayev, S. Bloom, A. Collow, S. Firth, G. Labow, G. Partyka, S. Pawson, O. Reale, S. D. Schubert, and M. Suarez, 2015: MERRA-2: Initial evaluation of the climate, Technical Report Series on Global Modeling and Data Assimilation, Vol43, NASA/TM-2015-1040606/Vol. 43.
- Donlon, C. J., M. Martin, J. Stark, J. Roberts-Jones, E. Fiedler, and W. Wimmer, 2012: The operational sea surface temperature and sea ice analysis (OSTIA) system. *Remote Sens. Environ.*, **116**, 140-158, doi: 10.1016/j.rse.2010.10.017.
- Dudok de Wit, T. G. Kopp, C. Fröhlich, and M. Schöll (2017), Methodology to create a new total solar irradiance record: Making a composite out of multiple data records, *Geophys. Res. Lett.*, **44**, 1196-1203, doi:10.1002/2016GL071866.
- Gelaro, R. and Coauthors, 2017: The Modern-Era Retrospective Analysis for Research and Applications, Version 2 (MERRA-2), *J. Climate*, **30**, 5419-5454, doi:10.1175/JCLI-D-16-0758.1.
- Hsu, N. C., Tsay, S.-C., King, M. D., and Herman, J. R.: Deep Blue Retrievals of Asian Aerosol Properties During ACE-Asia, *IEEE T. Geosci. Remote*, **44**, 3180–3195, <https://doi.org/10.1109/TGRS.2006.879540>, 2006.
- Johnson, G. C., J. M. Lyman, and N. G. Loeb. 2016. Improving estimates of Earth's energy imbalance. *Nature Climate Change*, **6**, 639-640, doi:10.1038/nclimate3043.
- Kato, S., and N. G. Loeb, 2003: Twilight irradiance reflected by the earth estimated from Clouds and the Earth's Radiant Energy System (CERES) measurements. *J. Climate*, **16**, 2646–2650.
- Kato, S., F. G. Rose, D. A. Rutan, T. E. Thorsen, N. G. Loeb, D. R. Doelling, X. Huang, W. L. Smith, W. Su, and S.-H. Ham, 2018: Surface irradiances of Edition 4.0 Clouds and the Earth's Radiant Energy System (CERES) Energy Balanced and Filled (EBAF) data product, *J. Climate*, **31**, 4501-4527, doi:10.1175/JCLI-D-17-0523.1.
- Kato, S., N. G. Loeb, F. G. Rose, S.-H. Ham, T. J. Thorsen, D. A. Rutan, W. F. Miller, T. E. Caldwell, D. R. Doelling, and S. Sun-Mack, 2025: Seamless continuity on CERES Energy Balanced and Filled (EBAF) surface radiation budget across multiple satellites, *J. Climate*, doi: 10.1175/JCLI-D-23-0568.1, in press.
- Levy, R. C., Mattoo, S., Munchak, L. A., Remer, L. A., Sayer, A. M., Patadia, F., and Hsu, N. C.: The Collection 6 MODIS aerosol products over land and ocean, *Atmos. Meas. Tech.*, **6**, 2989–3034, <https://doi.org/10.5194/amt-6-2989-2013>, 2013.
- Loeb, N. G., K. J. Priestley, D. P. Kratz, E. B. Geier, R. N. Green, B. A. Wielicki, P. O. R. Hinton, and S. K. Nolan, 2001: Determination of unfiltered radiances from the Clouds and the Earth's Radiant Energy System (CERES) instrument. *J. Appl. Meteor.*, **40**, 822–835.
- Loeb, N. G., S. Kato, and B. A. Wielicki, 2002: Defining top-of-atmosphere flux reference level for Earth Radiation Budget studies. *J. Climate*, **15**, 3301-3309.

- Loeb, N. G., D. R. Doelling, H. Wang, W. Su, C. Nguyen, J. G. Corbett, L. Liang, C. Mitrescu, F. G. Rose, and S. Kato, 2018: Clouds and the Earth's Radiant Energy System (CERES) Energy Balanced and Filled (EBAF) Top-of-Atmosphere (TOA) Edition-4.0 data product. *J. Climate*, **31**, 895-918, doi: 10.1175/JCLI-D-17-0208.1.
- Loeb, N. G. and Doelling, D. R., 2020: CERES Energy Balanced and Filled (EBAF) from Afternoon-Only Satellite Orbits. *Remote Sens.*, **12**, 1280. <https://doi.org/10.3390/rs12081280>.
- Loeb, N. G., D. R. Doelling, S. Kato, W. Su, P. E. Mlynyczak, and J. C. Wilkins, 2024: Continuity in top-of-atmosphere Earth radiation budget observations. *J. Climate*, **37**, 6093-6018, doi: 10.1175/JCLI-D-24-0180.1.
- Minnis, P., S. Sun-Mack, Y. Chen, F.-L. Chang, C. R. Yost, W. L. Smith, Jr., P. W. Heck, R. F. Arduini, S. T. Bedka, Y. Yi, G. Hong, Z. Jin, D. Painemal, R. Palikonda, B. R. Scarino, D. A. Spangenberg, R. A. Smith, Q. Z. Trepte, P. Yang, and Y. Xie, 2020: CERES MODIS cloud product retrievals for Edition 4, Part I: Algorithm changes. *IEEE Trans. Geosci. Remote Sens.*, **59**, 2744-2780, doi: <https://doi.org/10.1109/TGRS.2020.3008866>.
- Reynolds, R. W., T. M. Smith, C. Liu, D. B. Chelton, K. S. Casey, and M. G. Schlax, 2007: Daily High-Resolution-Blended Analyses for Sea Surface Temperature. *J. Climate*, **20**, 5473–5496, <https://doi.org/10.1175/2007JCLI1824.1>.
- Rutan, D., F. Rose, M. Roman, N. Manalo-Smith, C. Schaaf, and T. Charlock (2009), Development and assessment of broadband surface albedo from Clouds and the Earth's Radiant Energy System Clouds and Radiation Swath data product, *J. Geophys. Res.*, **114**, D08125, doi:10.1029/2008JD010669.
- Stephens, G. L., D. O'Brien, P. J. Webster, P. Pilewski, S. Kato, and J.-l. Li (2015), The albedo of Earth, *Rev. Geophys.*, **53**, 141–163, doi:10.1002/2014RG000449.
- Su, W., J. Corbett, Z. Eitzen, L. Liang, 2015a: Next-generation angular distribution models for top-of-atmosphere radiative flux calculation from CERES instruments: methodology. *Atmos. Meas. Tech.*, **8**(2), 611-632. doi:10.5194/amt-8-611-2015.
- Su, W., J. Corbett, Z. Eitzen, L. Liang, 2015b: Next-generation angular distribution models for top-of-atmosphere radiative flux calculation from CERES instruments: validation. *Atmos. Meas. Tech.*, **8**(8), 3297-3313. doi:10.5194/amt-8-3297-2015.
- Wilson, T.; Wu, A.; Shrestha, A.; Geng, X.; Wang, Z.; Moeller, C.; Frey, R.; Xiong, X., 2017: Development and Implementation of an Electronic Crosstalk Correction for Bands 27–30 in Terra MODIS Collection 6. *Remote Sens.*, **9**, 569. <https://doi.org/10.3390/rs9060569>.

7.0 Attribution

When referring to the CERES EBAF product, please include the data product and the data set version as "CERES_EBAF_Ed4.2" or "CERES_EBAF_Ed4.2.1."

The CERES Team has put forth considerable effort to remove major errors and to verify the quality and accuracy of this data. Please provide a reference to the following papers when you publish scientific results with the CERES EBAF_Ed4.2.

Loeb, N. G., D. R. Doelling, S. Kato, W. Su, P. E. Mlynczak, and J. C. Wilkins, 2024: Continuity in top-of-atmosphere Earth radiation budget observations. *J. Climate*, **37**, 6093-6018, doi: 10.1175/JCLI-D-24-0180.1.

Loeb, N. G., D. R. Doelling, H. Wang, W. Su, C. Nguyen, J. G. Corbett, L. Liang, C. Mitrescu, F. G. Rose, and S. Kato, 2018: Clouds and the Earth's Radiant Energy System (CERES) Energy Balanced and Filled (EBAF) Top-of-Atmosphere (TOA) Edition-4.0 Data Product. *J. Climate*, **31**, 895-918, doi: 10.1175/JCLI-D-17-0208.1.

PDF available at <https://journals.ametsoc.org/doi/pdf/10.1175/JCLI-D-17-0208.1>

Kato, S., N. G. Loeb, F. G. Rose, S.-H. Ham, T. J. Thorsen, D. A. Rutan, W. F. Miller, T. E. Caldwell, D. R. Doelling, and S. Sun-Mack, 2025: Seamless continuity on CERES Energy Balanced and Filled (EBAF) surface radiation budget across multiple satellites, *J. Climate*, doi: 10.1175/JCLI-D-23-0568.1, in press.

Kato, S., F. G. Rose, D. A. Rutan, T. E. Thorsen, N. G. Loeb, D. R. Doelling, X. Huang, W. L. Smith, W. Su, and S.-H. Ham, 2018: Surface irradiances of Edition 4.0 Clouds and the Earth's Radiant Energy System (CERES) Energy Balanced and Filled (EBAF) data product, *J. Climate*, **31**, 4501-4527, doi:10.1175/JCLI-D-17-0523.1.

PDF available at <https://journals.ametsoc.org/doi/pdf/10.1175/JCLI-D-17-0523.1>

When CERES data obtained via the CERES web site are used in a publication, we request the following acknowledgment be included: "These data were obtained from the NASA Langley Research Center CERES ordering tool at <https://ceres.larc.nasa.gov/data/>."

8.0 Feedback and Questions

For questions or comments on the CERES Data Quality Summary, contact the User and Data Services staff at the Atmospheric Science Data Center. For questions about the CERES subsetting/visualization/ordering tool at <https://ceres.larc.nasa.gov/data/> please email LaRC-CERES-Help@mail.nasa.gov.

9.0 Document Revision Record

The Document Revision Record contains information pertaining to approved document changes. The table lists the Version Number, the date of the last revision, a short description of the revision, and the revised sections.

Document Revision Record

Version Number	Date	Description of Revision	Section(s) Affected
V0	12/09/2022	• Original document.	All
V1	01/27/2023	• Added text regarding the new Ed4.2 surface fluxes.	Sec. 3.0 and 6.0
V2	01/02/2024	• Added text about the revised Ed4.2 fluxes.	Sec. 7.0
V3	05/03/2024	• Added Cautions and Helpful Hints section.	Sec. 7.0
V4	11/2024	• Added text and figures about new Ed4.2.1.	New Sec. 2.0 and 6.0. Other section numbers changed accordingly.
V5	4/9/2025	• Added text and figures about Ed4.2.1 surface fluxes. • Rearranged document.	All